STABILITY STUDIES OF SYNCHRONOUS-RELUCTANCE MACHINES

A Thesis

Presented to

the Faculty of Graduate Studies

University of Manitoba

In Partial Fulfillment

of the Requirements for the Degree

Master of Science

in

Electrical Engineering

by

Ho, Hing Yuen

February 1972

ACKNOWLEDGEMENT

The author wishes to express his deep gratitude to his thesis advisor, Professor R. W. Menzies, for suggesting the topic, as well as for his guidance and supervision. The author would also like to thank the National Research Council of Canada for their financial assistance during the preparation of this thesis.

ABSTRACT

Steady-state stability studies of a synchronous-reluctance machine operated from a variable frequency voltage source are performed by linearizing the equations describing the behavior of the machine during small perturbations about a steady-state operating point and then applying the Nyquist stability criterion.

An investigation of stability is made from the results of a digital computer study, and from experiments. Machine instability is revealed to occur mainly at low operating frequencies even though balanced, constant amplitude voltages are applied to the stator terminals.

TABLE OF CONTENTS

CHAPTER I

INTRODUCTION

A. GENERAL INTRODUCTION

Synchronous-reluctance machines have been considered as constant speed machines and their applications have been on constant frequency systems. Modern controlled semiconductors and their use in inverters have now made possible the application of synchronous-reluctance machines in controlled variable speed drives. Control of both speed and direction of rotation of the machine has been made practical by controlling the frequency and voltage, and phase sequence respectively. As controlled drives begin to be widely employed in industrial and traction applications, analysis of machine stability over the frequency range is needed.

In the stability analysis the behavior of the synchronous-reluctance machine is described by the basic equations similar to those employed in synchronous machine theory. Transformation to the d-q-0 axes fixed on the rotor is performed. The equations obtained by allowing small changes about a steady-state operating point are nonlinear. To reduce the complexity, these equations are linearized, and machine stability is predicted applying the Nyquist stability criterion for various speeds and different system parameters. Experimental tests are performed and compared to the predicted results on the stability of the machines.

It is shown that the machine stability is dependent on both

the amplitude and frequency of the applied voltages, the system inertia, and the electrical parameters of the machine. Machine instability occurs with balanced applied voltages which are independent of load currents. Instability is therefore not due to an interaction between the machine and the voltage source, and instability is found to be inherent at low frequencies (machine speeds).

B. ALTERNATE APPROACHES

Stability analysis of electric machines has been traditionally performed by analog computers. Attempts by the author to study the steady-state stability of the synchronous-reluctance machines at variable speeds were made using the analog computer. However, the simulation requirements are not met due to the large number of multipliers needed to simulate the approximately rectangular voltages from the inverter. If the supply voltages are assumed to be sinusoidal, analog computer techniques would produce modes of machine stability very close to those predicted by the digital computer program because the system models are the same for both cases.

Other familiar techniques involved in the investigation of machine steady-state stability are the root locus method and Routh-Hurwitz method. The root locus method is inconvenient because the method requires immense work in plotting the root loci of a very high order system (a minimum order of 4). The Routh-Hurwitz criterion gives the same results as the Nyquist criterion, but the digital computer program for the Nyquist criterion is more easily programmed and the results more readily show the machine stability modes (See Chapter IV,

Section (C)).

Another method recently used by Lawrenson is the D-decomposition technique[1]. This method also detects machine instability at higher supply frequencies. However, machine tests performed by the author of this thesis did not exhibit unstable steady-state operation with the chosen machine parameters and operating conditions at high frequencies. Analyses of synchronous machine stability have also been made employing phase space approach[2], Volterra series approach[3], and Liapunov stability approach[4]. These methods are very effective in analyzing nonlinear systems, and in these analyses linearization of the equations describing the behavior of the machine is not used. These methods can be extended to study the stability of synchronous-reluctance machines. But in this thesis the analysis employing Nyquist stability criterion also serves the same purpose as far as steady-state stability is concerned, and the method is fairly simple.

CHAPTER II

BASIC EQUATIONS

The generalized machine theory is employed to describe the transient and steady-state performance of an idealized synchronous-reluctance machine. In the development of this theory the following assumptions are made:

(1) Each stator winding is distributed so as to produce a sinusoidal MMF wave along the air gap.

(2) Irregularity of the cylindrical magnetic structure of the stator introduced by the presence of slots produce negligible variations in the self-inductances of the rotor windings.

(3) Saturation of the magnetic circuit is neglected.

(4) Balanced sinusoidal voltages are supplied from a zero-impedance source.

The idealized machine considered is a four-pole, three-phase synchronous-reluctance machine as shown in Figure 1. The analysis can be extended to machines with any number of pole pairs. The amortisseur windings are embedded in the rotor which is made cylindrical in shape. The amortisseur windings are very useful in damping out oscillations in rotor speed, and in providing the machine with a self-starting capability, the torque for which is produced by induction.

(A) FUNDAMENTAL EQUATIONS

The appropriate voltage equation for each of the windings, with the appropriate subscript, that is, as, bs, cs, qr, or dr, can be expressed as

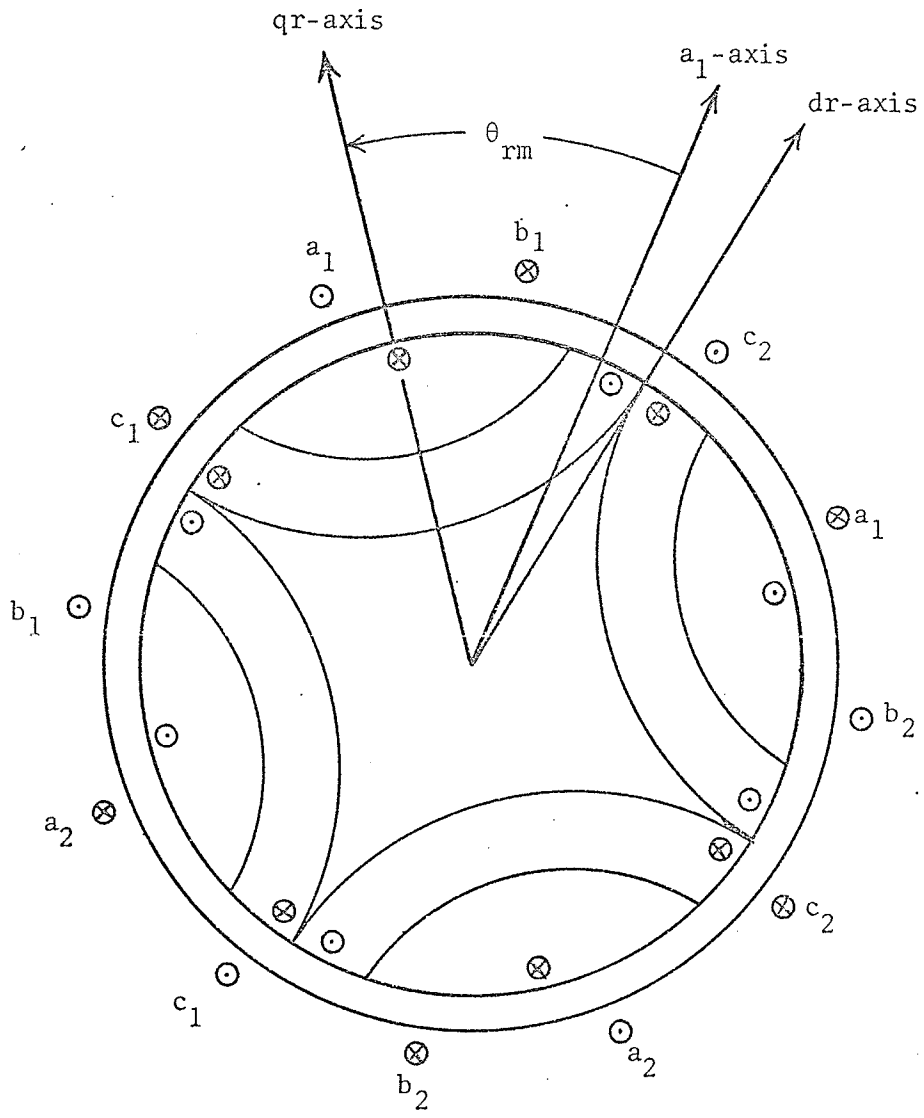

Figure 1. Four-pole, 3-phase Synchronous-reluctance machine

$$v = p\lambda + ri \tag{1}$$

The flux linkages may be expressed as

$$\begin{bmatrix} \lambda_{as} \\ \lambda_{bs} \\ \lambda_{cs} \\ \lambda_{dr} \\ \lambda_{qr} \end{bmatrix} = \begin{bmatrix} L_{asas} & L_{bsas} & L_{csas} & L_{dras} & L_{qras} \\ L_{asbs} & L_{bsbs} & L_{csbs} & L_{drbs} & L_{qrbs} \\ L_{ascs} & L_{bscs} & L_{cscs} & L_{drcs} & L_{qrcs} \\ L_{asdr} & L_{bsdr} & L_{csdr} & L_{drdr} & L_{qrdr} \\ L_{asqr} & L_{bsqr} & L_{csqr} & L_{drqr} & L_{qrqr} \end{bmatrix} X \begin{bmatrix} i_{as} \\ i_{bs} \\ i_{cs} \\ i_{dr} \\ i_{qr} \end{bmatrix} \tag{2}$$

By the assumptions we have made the self-inductances of the rotor circuits (dr and qr) are constants, independent of θ_r. Because of the symmetry of the rotor, the stator self-inductances and the mutual inductances between stator windings are expressed as a series of cosines of even harmonics of angle θ_r [7, pp. 10-12]. With the sinusoidal winding distribution only the first two terms of each series are

significant and other terms of the series are neglected. Because only sinusoidal MMF is produced along the air gap it is realized that stator-to-rotor mutual inductances vary sinusoidally with θ_r. The following equations describe the inductances which were given in (2).

Stator self-inductances:

$$L_{asas} = L_{ls} + L_{s0} - L_{s1} \cos (2\theta_r) \tag{3}$$

$$L_{bsbs} = L_{ls} + L_{s0} - L_{s1} \cos 2(\theta_r - 2\pi/3) \tag{4}$$

$$L_{cscs} = L_{ls} + L_{s0} - L_{s1} \cos 2(\theta_r + 2\pi/3). \tag{5}$$

Rotor self-inductances:

$$L_{drdr} = L_{ldr} + L_{dr0} \tag{6}$$

$$L_{qrqr} = L_{lqr} + L_{qr0}. \tag{7}$$

Stator-to-stator mutual inductances:

$$L_{asbs} = L_{bsas} = -1/2\, L_{s0} - L_{s1} \cos 2(\theta_r - \pi/3) \tag{8}$$

$$L_{ascs} = L_{csas} = -1/2\, L_{s0} - L_{s1} \cos 2(\theta_r + \pi/3) \tag{9}$$

$$L_{bscs} = L_{csbs} = -1/2\, L_{s0} - L_{s1} \cos 2(\theta_r + \pi). \tag{10}$$

Rotor-to-rotor mutual inductances:

$$L_{drqr} = L_{qrdr} = 0. \tag{11}$$

Stator-to-rotor mutual inductances:

$$L_{asdr} = L_{dras} = L_{sdr} \sin \theta_r \tag{12}$$

$$L_{asqr} = L_{qras} = L_{sqr} \cos \theta_r \tag{13}$$

$$L_{bsdr} = L_{drbs} = L_{sdr} \sin (\theta_r - 2\pi/3) \tag{14}$$

$$L_{bsqr} = L_{qrbs} = L_{sqr} \cos (\theta_r - 2\pi/3) \tag{15}$$

$$L_{csdr} = L_{drcs} = L_{sdr} \sin (\theta_r + 2\pi/3) \tag{16}$$

$$L_{csqr} = L_{qrcs} = L_{sqr} \cos (\theta_r + 2\pi/3). \tag{17}$$

In the above equations the subscripts ls, ldr, lqr denote the leakage inductances of the stator, dr and qr windings, respectively. The constant terms and the coefficients of the second terms of the Fourier Series are denoted by s0 and s1 respectively.

(B) TRANSFORMATION OF STATOR QUANTITIES TO REFERENCE FRAME FIXED ON ROTOR

To simplify the mathematical procedure in the analysis of synchronous-reluctance machines the stator and rotor variables are transformed to a common frame of reference fixed in the rotor. In this reference frame the voltage equations do not contain any time varying coefficients at synchronous speed. The stator variables are transformed to the reference frame fixed on the rotor by

$$f_{qs} = \sqrt{2/3} \left[f_{as} \cos \theta_r + f_{bs} \cos (\theta_r - 2\pi/3) + f_{cs} \cos (\theta_r + 2\pi/3) \right] \tag{18}$$

$$f_{ds} = \sqrt{2/3} \left[f_{as} \sin \theta_r + f_{bs} \sin (\theta_r - 2\pi/3) + f_{cs} \sin (\theta_r + 2\pi/3) \right] \tag{19}$$

$$f_{0s} = \sqrt{1/3}\ [f_{as} + f_{bs} + f_{cs}] \tag{20}$$

In the above three equations the variable f can represent either voltage, current, or flux-linkage. As the stator is a symmetrical, balanced three-phase system, the third transform variable f_{0s} is zero.

After referring the rotor quantities to the stator windings by the appropriate turns ratio and transforming the stator voltages and currents to the reference frame fixed in the rotor where the symmetry exists, the voltage equations may be expressed as

$$v_{qs} = p\lambda_{qs} + \lambda_{ds}\, p\theta_r + r_s i_{qs} \tag{21}$$

$$v_{ds} = p\lambda_{ds} - \lambda_{qs}\, p\theta_r + r_s i_{ds} \tag{22}$$

$$v_{qr}' = p\lambda_{qr} + r_{qr}'\, i_{qr}' \tag{23}$$

$$v_{dr}' = p\lambda_{dr} + r_{dr}'\, i_{dr}' \tag{24}$$

where $$\lambda_{qs} = L_{ls}\, i_{qs} + L_{aq}\, (i_{qs} + i_{qr}') \tag{25}$$

$$\lambda_{ds} = L_{ls}\, i_{ds} + L_{ad}\, (i_{ds} + i_{dr}') \tag{26}$$

$$\lambda_{qr}' = L_{lqr}'\, i_{qr}' + L_{aq}\, (i_{qs} + i_{qr}') \tag{27}$$

$$\lambda_{dr}' = L_{ldr}'\, i_{dr}' + L_{ad}\, (i_{ds} + i_{dr}') \tag{28}$$

and where

$$\begin{aligned} L_{ad} &= 3/2\ (L_{s0} + L_{s1}) \\ &= 3/2\ (N_s/N_{dr})\ L_{sdr} \\ &= 3/2\ (N_s/N_{dr})^2\ L_{dr0} \end{aligned} \tag{29}$$

$$L_{aq} = 3/2\ (L_{s0} - L_{s1})$$

$$= 3/2\ (N_s/N_{qr})\ L_{sqr}$$

$$= 3/2\ (N_s/N_{qr})^2\ L_{qr0} \tag{30}$$

$$L_{1dr}' = 3/2\ (N_s/N_{dr})^2\ L_{1dr} \tag{31}$$

$$r_{dr}' = 3/2\ \ (N_s/N_{dr})^2 r_{dr} \tag{32}$$

$$i_{dr}' = 2/3\ (N_{dr}/N_s)\ i_{dr} \tag{33}$$

$$v_{dr}' = (N_s/N_{dr})\ v_{dr}. \tag{34}$$

The equations relating qr and qr' quantities are similar to those relating dr and dr' quantities, and N denotes the number of turns of the corresponding windings. The primed rotor quantities are rotor quantites referred to the stator windings.[8]

CHAPTER III

APPLICATION OF SMALL-DISPLACEMENT THEORY TO SYNCHRONOUS-RELUCTANCE MACHINES

The small-displacement theory enables us to establish linear relationships between the machine variables for small changes about a steady-state operating point. The small-displacement equations are not valid for large excursions of the variables from the operating point, but in conjunction with the Nyquist stability criterion the linearized relationships offer an approach to investigate the machine stability.

A. STEADY-STATE OPERATION

The rotor circuits of the synchronous-reluctance machine are short-circuited ($v_{qr} = v_{dr} = 0$). During balanced, steady-state operation wherein the reluctance machine rotates at an electrical angular velocity corresponding to that of the applied voltages, the rotor currents (i_{qr} and i_{dr}) are zero. The equations describing the steady-state operation can be obtained from (21) through (28) by setting

$$v_{dr} = v_{qr} = i_{dr} = i_{qr} = 0$$

and are expressed as

$$V \cos \delta_0 = X_{ds} f_r i_{ds0} + r_s i_{qs0} \qquad (35)$$

$$V \sin \delta_0 = - X_{qs} f_r i_{qs0} + r_s i_{ds0} \quad (36)$$

where V denotes the amplitude of the balanced applied stator voltages, the letter 0 in the subscript denotes steady-state quantities and

$$X_{ds} = \omega_e \times (L_{ls} + L_{ad}) = X_{ls} + X_{ad} \quad (37)$$

$$X_{qs} = \omega_e (L_{ls} + L_{aq}) = X_{ls} + X_{aq} \quad (38)$$

$$\delta_0 = \theta_r - \omega_{r0} t \quad (39)$$

$$f_r = \omega_{r0}/\omega_e. \quad (40)$$

For motor action the steady-state rotor load angle δ_0 is negative. The electrical angular velocity ω_e is the chosen base frequency which is 60 Hz. ω_{r0} is the steady-state electrical angular velocity of the rotor which is determined by the applied stator voltages.

The steady-state torque for a 4-pole, three-phase machine is given by

$$T_{e0} = 3/2 \times P/\omega_e \times (X_{ds} - X_{qs}) i_{ds0} i_{qs0}. \quad (41)$$

where $P = 2$ for a 4-pole machine.

Equation (21) through (28) can be expressed in matrix form as

$$\begin{bmatrix} \overline{v}_{qs0} \\ v_{ds0} \\ v_{qr0}' \\ v_{dr0}' \end{bmatrix} = \begin{bmatrix} \overline{V} \cos \delta_0 \\ V \sin \delta_0 \\ 0 \\ 0 \end{bmatrix} =$$

$$\begin{bmatrix} r_s + \frac{p}{\omega_e}X_{qs} & \frac{\omega_{r0}}{\omega_e}X_{ds} & \frac{p}{\omega_e}X_{aq} & \frac{\omega_{r0}}{\omega_e}X_{ad} \\ -X_{qs}\frac{\omega_{r0}}{\omega_e} & r_s + \frac{p}{\omega_e}X_{ds} & -X_{aq} f_r & \frac{p}{\omega_e}X_{ad} \\ \frac{p}{\omega_e}X_{aq} & 0 & r_{qr}' + \frac{p}{\omega_e}X_{qr}' & 0 \\ 0 & \frac{p}{\omega_e}X_{ad} & 0 & r_{dr}' + \frac{p}{\omega_e}X_{dr}' \end{bmatrix} \times \begin{bmatrix} i_{qs0} \\ i_{ds0} \\ 0 \\ 0 \end{bmatrix} \quad (42)$$

By letting p be zero in (42) we can solve for i_{qs0} and i_{ds0}, and consequently T_{e0} from (41):

$$i_{qs0} = (r_s V \cos \delta_0 - f_r X_{ds} V \sin \delta_0) / (r_s^2 + f_r^2 X_{ds} X_{qs}) \quad (43)$$

$$i_{ds0} = (r_s V \sin \delta_0 - f_r X_{qs} V \sin \delta_0) / (r_s^2 + f_r^2 X_{ds} X_{qs}) \quad (44)$$

$$\begin{aligned} T_{e0} = &\left[\frac{3}{\omega_e}(X_{ds} - X_{qs}) V^2 / (r_s^2 + f_r^2 X_{ds} X_{qs})\right] \\ &\left[r_s^2 \sin 2\delta_0 - f_r r_s X_{ds} + f_r r_s X_{ds} \cos 2\delta_0\right. \\ &+ f_r r_s X_{qs} + f_r r_s X_{qs} \cos 2\delta_0 \\ &\left. - f_r^2 X_{ds} X_{qs} \sin 2\delta_0\right] \end{aligned} \quad (45)$$

B. SMALL-DISPLACEMENT FROM STEADY-STATE OPERATING POINT

By allowing the variables in (42) to change by small amounts about the initial steady-state operating point, we have

$$\begin{bmatrix} V\cos(\delta_0 + \Delta\delta) \\ V\sin(\delta_0 + \Delta\delta) \\ 0 \\ 0 \end{bmatrix} =$$

$$\begin{bmatrix} r_s + \frac{p}{\omega_e}X_{qs} & X_{ds}\left(\frac{\omega_{r0} + \Delta\omega_r}{\omega_e}\right) & \frac{p}{\omega_e}X_{aq} & X_{ad}\left(\frac{\omega_{r0} + \Delta\omega_r}{\omega_e}\right) \\ -X_{qs}\left(\frac{\omega_{r0} + \Delta\omega_r}{\omega_e}\right) & r_s + \frac{p}{\omega_e}X_{ds} & -X_{aq}\left(\frac{\omega_{r0} + \Delta\omega_r}{\omega_e}\right) & \frac{p}{\omega_e}X_{ad} \\ \frac{p}{\omega_e}X_{aq} & 0 & r_{qr}' + \frac{p}{\omega_e}X_{qr}' & 0 \\ 0 & \frac{p}{\omega_e}X_{ad} & 0 & r_{dr}' + \frac{p}{\omega_e}X_{dr}' \end{bmatrix}$$

$$x \begin{bmatrix} i_{qs0} + \Delta i_{qs} \\ i_{ds0} + \Delta i_{ds} \\ \Delta i_{qr}' \\ \Delta i_{dr}' \end{bmatrix} \qquad (46)$$

where

$$\Delta\omega_r = p\Delta\delta \tag{47}$$

$$X_{dr}' = X_{ldr}' + X_{ad} = \omega_e(L_{ldr}' + L_{ad}) \tag{48}$$

$$X_{qr}' = X_{lqr}' + X_{aq} = \omega_e(L_{lqr}' + L_{aq}). \tag{49}$$

For small changes in the rotor angle δ the following approximations hold:

$$V \cos(\delta_0 + \Delta\delta) \approx V \cos\delta_0 - V(\sin\delta_0)\Delta\delta \tag{50}$$

$$V \sin(\delta_0 + \Delta\delta) \approx V \sin\delta_0 + V(\cos\delta_0)\Delta\delta \tag{51}$$

By substituting (50) and (51) into (46) and then subtracting the resultant matrix from (42) we can eliminate all the terms which describe the steady-state mode of operation, thus we then obtain the equations:

$$\begin{bmatrix} -V(\sin\delta_0)\Delta\delta - X_{ds} i_{ds0} \dfrac{\Delta\omega_r}{\omega_e} \\ V(\cos\delta_0)\Delta\delta + X_{qs} i_{qs0} \dfrac{\Delta\omega_r}{\omega_e} \\ 0 \\ 0 \end{bmatrix} =$$

$$\begin{bmatrix} r_s + \frac{p}{\omega_e}X_{qs} & X_{ds}\frac{\omega_{r0}}{\omega_e} & \frac{p}{\omega_e}X_{aq} & X_{ad}\left(\frac{\omega_{r0}+\Delta\omega_r}{\omega_e}\right) \\ -X_{qs}\frac{\Delta\omega_r}{\omega_e} & r_s + \frac{p}{\omega_e}X_{ds} & -X_{aq}\left(\frac{\omega_{r0}+\Delta\omega_r}{\omega_e}\right) & \frac{p}{\omega_e}X_{ad} \\ \frac{p}{\omega_e}X_{aq} & 0 & r_{qr}' + \frac{p}{\omega_e}X_{qr}' & 0 \\ 0 & \frac{p}{\omega_e}X_{ad} & 0 & r_{dr}' + \frac{p}{\omega_e}X_{dr}' \end{bmatrix} x$$

$$\begin{bmatrix} \Delta i_{qs} \\ \Delta i_{ds} \\ \Delta i_{qr}' \\ \Delta i_{dr}' \end{bmatrix} \qquad (52)$$

From (52) the rotor currents can be expressed in terms of stator currents:

$$\Delta i_{qr}' = \left(-\frac{p}{\omega_e}X_{aq}\,\Delta i_{qs}\right) / \left(r_{qr}' + \frac{p}{\omega_e}X_{qr}'\right) \qquad (53)$$

$$\Delta i_{dr}' = \left(-\frac{p}{\omega_e}X_{ad}\,\Delta i_{ds}\right) / \left(r_{dr}' + \frac{p}{\omega_e}X_{dr}'\right). \qquad (54)$$

By substituting (53) and (54) into (52) and neglecting second order differences, we obtain the following small-displacement equations:

$$\begin{bmatrix} -\left(V\sin\delta_0 - \frac{p}{\omega_e}X_{ds}\,i_{ds0}\right) \\ V\cos\delta_0 + \frac{p}{\omega_e}X_{qs}\,i_{qs0} \end{bmatrix} \Delta\delta =$$

$$\begin{bmatrix} r_s + \frac{p}{\omega_e} X_{qs} - \frac{(\frac{p}{\omega_e})^2 X_{aq}^2}{r_{qr}' + \frac{p}{\omega_e} X_{qr}'} & X_{ds} f_r - \frac{\frac{p}{\omega_e} f_r X_{ad}^2}{r_{dr}' + \frac{p}{\omega_e} X_{dr}'} \\ - X_{qs} f_r + \frac{\frac{p}{\omega_e} f_r X_{aq}^2}{r_{qr}' + \frac{p}{\omega_e} X_{qr}'} & r_s + \frac{p}{\omega_e} X_{ds} - \frac{(\frac{p}{\omega_e})^2 X_{ad}^2}{r_{dr}' + \frac{p}{\omega_e} X_{dr}'} \end{bmatrix} x \begin{bmatrix} \Delta i_{qs} \\ \Delta i_{ds} \end{bmatrix} \tag{55}$$

During small changes about a steady-state operating point the torque expression becomes

$$\begin{aligned} T_{e0} + \Delta T_{e0} = {} & \frac{3}{\omega_e} (X_{ds} - X_{qs}) (i_{ds0} + \Delta i_{ds}) (i_{qs0} + \Delta i_{qs}) \\ & + \frac{3}{\omega_e} X_{ad} (i_{qs0} + \Delta i_{qs}) \Delta i_{dr}' \\ & - \frac{3}{\omega_e} X_{aq} (i_{ds0} + \Delta i_{ds}) \Delta i_{qr}' \end{aligned} \tag{56}$$

Neglecting second-order differences and expressing the rotor currents in terms of stator currents, and then eliminating the steady-state torque expression (41) from (56), the small-displacement torque expression becomes

$$\Delta T_e = \frac{3}{\omega_e} \left[(X_{ds} - X_{qs}) (i_{ds0} \Delta i_{qs} + i_{qs0} \Delta i_{ds}) - \right.$$

$$\left.\frac{\frac{p}{\omega_e}X_{ad}^2 i_{qs0}}{r_{dr}' + \frac{p}{\omega_e}X_{dr}'}\Delta i_{ds} + \frac{\frac{p}{\omega_e}X_{aq}^2 i_{ds0}}{r_{qr}' + \frac{p}{\omega_e}X_{qr}'}\Delta i_{qs}\right] \tag{57}$$

When (55) is solved for Δi_{qs} and Δi_{ds} and the results substituted into (57), the following expression can be obtained (See Appendix B):

$$\Delta T_e = G(p)\Delta\delta. \tag{58}$$

This equation denotes a linear, small-displacement relationship between the electromagnetic torque and the rotor load angle.

To simplify computation all quantities are converted to per unit quantities by selecting the base voltage, current, and frequency to correspond to the rating of the machine.

The small-displacement equation describing the dynamics of the mechanical system during small changes about an initial operating speed can be obtained from the steady-state electromagnetic torque equation by allowing small changes in the variables:

$$\underset{\sim}{T_{L0}} + \underset{\sim}{\Delta T_L} = \underset{\sim}{T_{e0}} + \underset{\sim}{\Delta T_e} - \underset{\sim}{J}\,\underset{\sim}{p}\,\underset{\sim}{\nu} \tag{59}$$

where the notation $\sim$ denotes per unit quantities. Since in the steady-state, $T_{L0} = T_{e0}$ where T_{L0} is the steady-state load torque including friction and windage losses, and since $\underset{\sim}{\nu} = \underset{\sim}{\omega_r}$, the small-displacement equation obtained from (59) is

$$\underset{\sim}{\Delta T_L} = \underset{\sim}{\Delta T_e} - \underset{\sim}{J}\,\underset{\sim}{p}\,\underset{\sim}{\omega_r} \tag{60}$$

or

$$\underset{\sim}{\Delta T_L} = \underset{\sim}{\Delta T_e} - \frac{2H}{\omega_e}p^2\Delta\delta. \tag{61}$$

CHAPTER IV

METHOD OF DETERMINING MACHINE STABILITY

A. APPLICATION OF NYQUIST STABILITY CRITERION

From equations (58) and (61) we can construct the system block diagram which is shown in Figure 2. Since the system which approximately represents the synchronous-reluctance machine is linear, we can investigate the stability of the synchronous-reluctance machine as if it was a linear feedback system, in the frequency domain employing the Nyquist stability criterion.

The open-loop transfer function of the system in Figure 2 is expressed as

$$F(p) = - \frac{\omega_e \, G(p)}{2 H p^2} \tag{62}$$

By replacing p by the Laplace variable s (62) becomes

$$F(s) = - \frac{\omega_e \, G(s)}{2 H s^2} \tag{62a}$$

By setting s in (62a) equal to $j\nu$, the open-loop transfer function becomes

$$F(j\nu) = + \frac{\omega_e \, G(j\nu)}{2 H \nu^2} \tag{63}$$

Writing $G(j\nu) = a(\nu) + j\, b(\nu)$ (61) becomes

$$F(j\nu) = \frac{\omega_e}{2 H \nu^2} [a(\nu) + j\, b(\nu)] \tag{64}$$

The stability of the closed-loop system can be determined from

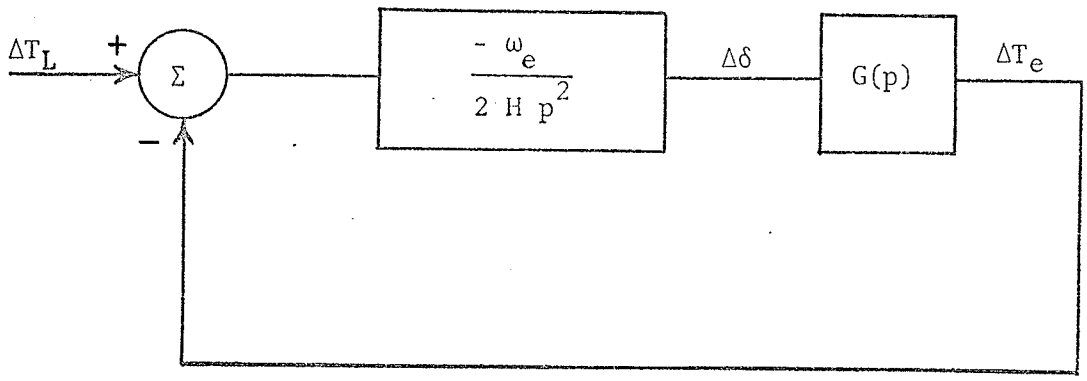

Figure 2. Small-displacement closed-loop system.

the locus of $F(j\nu)$ as ν varies from $-\infty$ to $+\infty$. The Nyquist stability criterion states that a feedback system is stable if and only if the locus of $F(j\nu)$ does not encircle the $(-1, 0)$ point when the number of poles of $F(s)$ in the right-hand s-plane is zero [6]. For the synchronous-reluctance machine the expression $F(s)$ does not have poles in the right-hand s-plane, therefore the feedback system is stable only if the locus of $F(j\nu)$ does not pass through or encircle the $(-1, 0)$ point.

The expression $G(j\nu)$ is given in Appendix C.

By analysing the locus of the frequency response of the system which represents the synchronous-reluctance machine under small changes about its steady-state operating point, it is fairly easy to predict the machine stability when balanced voltages of constant rms value and constant frequency are applied to the stator windings.

With the appropriate machine parameters and steady-state operating conditions, the plot of $F(j\nu)$ in the Nyquist diagrams are similar to the one shown in Figure 3(a). Since the locus of $F(j\nu)$ is symmetrical about the real axis we can obtain only the locus of $F(j\nu)$ as ν is varied from 0 to $+\infty$ and then reflect it about the real axis to obtain the complete contour. The three plots of $F(j\nu)$ shown in Figure 3(b) correspond to the initial operating points:

Machine operated at rated stator voltage (1 p.u. voltage), $T_{eo} = 0$;

and (a) machine speed of 123 electrical radians per second ($f_r = 0.36$),

(b) machine speed of 226 electrical radians per second ($f_r = 0.60$),

(c) machine speed of 368 electrical radians per second ($f_r = 0.96$).

The machine tested was designated ALACN (See Chapter V, Section (A)). With the operating conditions of point (a), the locus of $F(j\nu)$ encircles the (-1, 0) point as ν varies from $-\infty$ to $+\infty$. The system is unstable. At the initial operating conditons of point (b) the locus of $F(j\nu)$ passes through the (-1, 0) point, suggesting that the machine is operating on its stability boundary and the machine would display sustained oscillations when it is subjected to a small disturbance. At the initial operating conditions of point (c) the locus of $F(j\nu)$ fails to encircle or pass through the (-1, 0) point; the system is stable.

Thus the small-displacement theory enables us to determine machine stability under various initial operating conditions. The machine used in the experiment was found to be quite stable when loaded with a mechanical load of noticeable magnitude less than the rated value; the mechanical load helps in damping out the rotor oscillations caused by small disturbances to the machine. These small disturbances may be a change in the supply voltage, or mechanical load. Therefore we conducted our tests on the machine which was not loaded to locate the stability boundary for the worst case --- that of the unloaded machine.

B. THE DIGITAL COMPUTER PROGRAM

The digital computer is programmed appropriately to give the locus points of $F(j\nu)$ as ν is varied from 0.08 radians per second

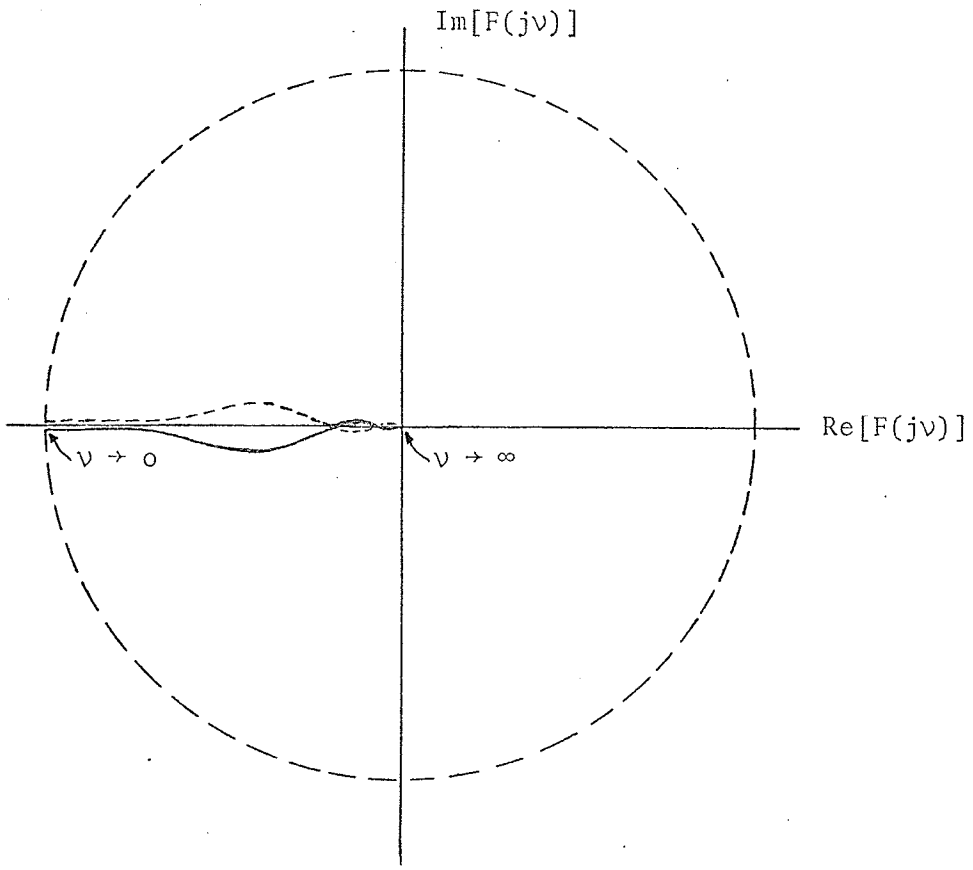

(a) Complete Contour

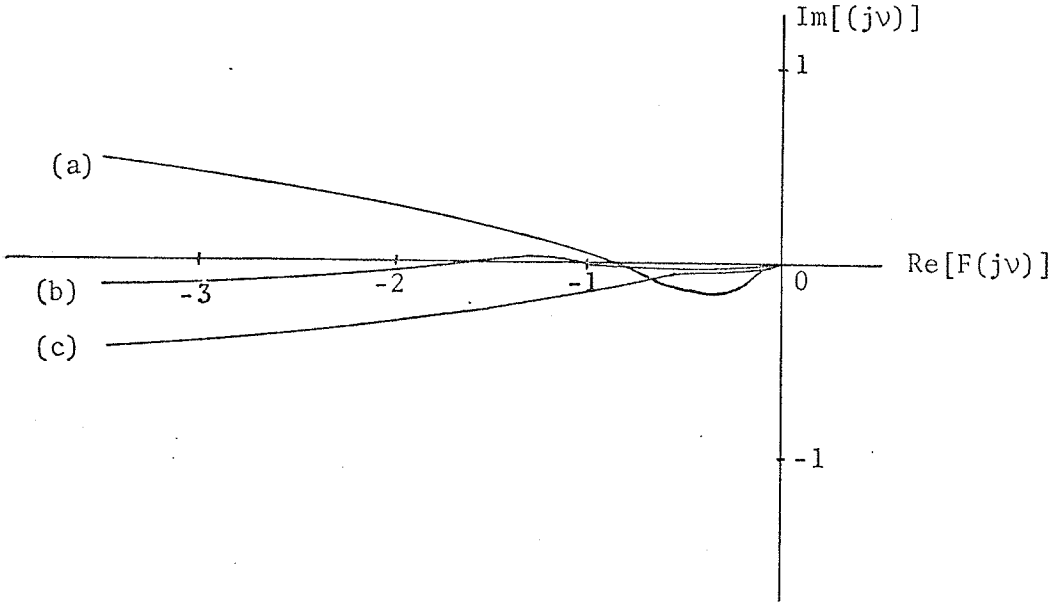

(b) Region Near the (-1, 0) Point

Figure 3. Nyquist Diagrams for the plot of F(jν).

to 138 radians per second for each initial operating point. By examining where the locus crosses the $Re[F(j\nu)]$ axis, that is, when $Im[f(j\nu)]$ is zero, we determine whether the machince is stable or unstable, or the machine is operating at the stability boundary conditions.

The above range of ν is chosen because the natural frequency of oscillations of the rotor is always less than the frequency of the applied voltage, and because this range of ν produces loci near the (-1, 0) point on the Nyquist diagram, giving sufficient information for the determination of the stability of the machine.

The digital computer program is shown in Appendix D. This computer program can be modified to give any initial operating conditions by inserting a T_{e0} loop for the machine load, or/and by varying the machine parameters.

CHAPTER V

TECHNICAL CONSIDERATIONS

A. MACHINES TESTED

The machine stability tests were performed on the same Westinghouse 3-horsepower Life Line 4-pole induction motor stator, with one of the following three rotors[35]:

(1) Axially laminated anisotropic narrow-pole-pitched rotor, denoted as ALASN;

(2) Axially laminated anisotropic broad-pole-pitched rotor, denoted as ALASB;

(3) Axially laminated anisotropic with copper foil inter-leaving narrow-pole-pitched rotor, denoted as ALACN.

With the corresponding rotor in place the synchronous-reluctance machine has the parameter values as shown in Table 1. (Refer to Chapter V, Section (c)).

B. VOLTAGE SOURCE AND EFFECTS OF STEP-UP TRANSFORMERS

Since there is no access to a three-phase voltage source the magnitude and frequency of which can be varied to the desired values, a Ward-Leonard system with elementary feedback control was set up to drive a 3-phase synchronous generator at variable speed. The amplitude of the generated voltage per cycle from this synchronous machine was controlled by adjusting its field excitation voltage while the frequency was controlled by adjusting the speed at which the generator was being

Table 1. Machine parameters.

Rotor			ALACN	ALASN	ALASB	ALASB
J_r(kg-m^2)			0.01647	0.01839	0.01876	0.10097
r_s (Ω)		V_m = 0.866	0.8063	0.8063	0.8063	0.8063
		V_m = 1.000	0.8262	0.8262	0.8262	0.8262
		V_m = 1.133	0.8780	0.8780	0.8780	0.8780
X_{ls} (Ω)		V_m = 0.866	0.8515	0.8515	0.8515	0.8515
		V_m = 1.000	0.8468	0.8468	0.8468	0.8468
		V_m = 1.133	0.9028	0.9028	0.9028	0.9028
X_{ldr}' (Ω)			0.7125	1.3280	0.5724	0.5724
X_{lqr}' (Ω)			0.9037	0.8161	1.0254	1.0254
r_{dr}' (Ω)			0.4352	1.0518	0.8468	0.8468
r_{qr}' (Ω)			0.8693	0.8227	1.0559	1.0559
X_{ad} (Ω)	PE*		23.70	21.45	20.45	20.45
	OP**	V_m = 0.866	12.90	13.20	13.60	13.60
		V_m = 1.000	8.00	10.50	10.00	10.00
		V_m = 1.133	5.40	8.20	6.70	6.70
X_{aq} (Ω)	PE*		2.20	2.20	3.20	3.20
	OP**	V_m = 0.866	1.70	2.40	3.20	3.20
		V_m = 1.000	1.70	2.40	3.20	3.20
		V_m = 1.133	1.70	2.40	3.20	3.20

* PE denotes peak value; ** OP denotes operating value.

driven. Hence a 3-phase voltage source of variable frequency and variable magnitude of volt-per-cycle was obtained. These balanced voltages were applied to the stator windings of the synchronous-reluctance machine. However, this whole system became unstable when there were very small oscillations in the synchronous-reluctance machine. That is, the voltage source interacts with the synchronous-reluctance machine, and the synchronous generator coupled to the Ward-Leonard system was not able to supply balanced, sinusoidal voltages which are independent of the load currents.

The tests were therefore performed using a three-phase static converter with variable frequency control. The magnitude of the output voltages of the converter was approximately proportional to the frequency, i.e., $V \simeq f_r V_m$ in per unit quantities, with resistance compensated characteristics. The output voltages are approximately rectangular instead of sinusoidal, as shown in Figure 4.

To obtain the desired value of rated voltage it is necessary to step up the output voltages from the converter using three power transformers, one for each phase. These transformers inherently introduce winding resistances and leakage reactances. Therefore the resistances, and leakage reactances of the transformers must be included as part of the stator resistances and leakage reactances respectively. The q-axis equivalent-circuit of the resultant circuit is shown in Figure 5(b). The resultant d-axis equivalent-circuit is also realized by an identical method. The magnetizing impedances of the transformers are neglected because the voltage regulation of each transformer is dependent mainly on the winding resistance and leakage reactance.

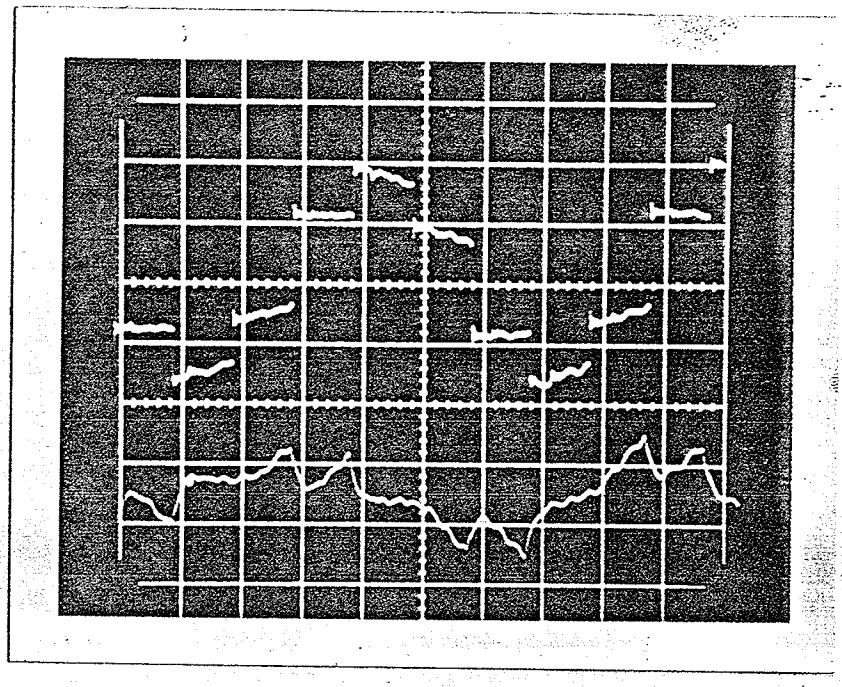

(a) Operation at 16.7 Hz. Horizontal scale: 10 ms/div.
Voltage (curve at top): Vert. scale: 50 V/div.
Current (curve at bottom): Vert. scale: 20 A/div.

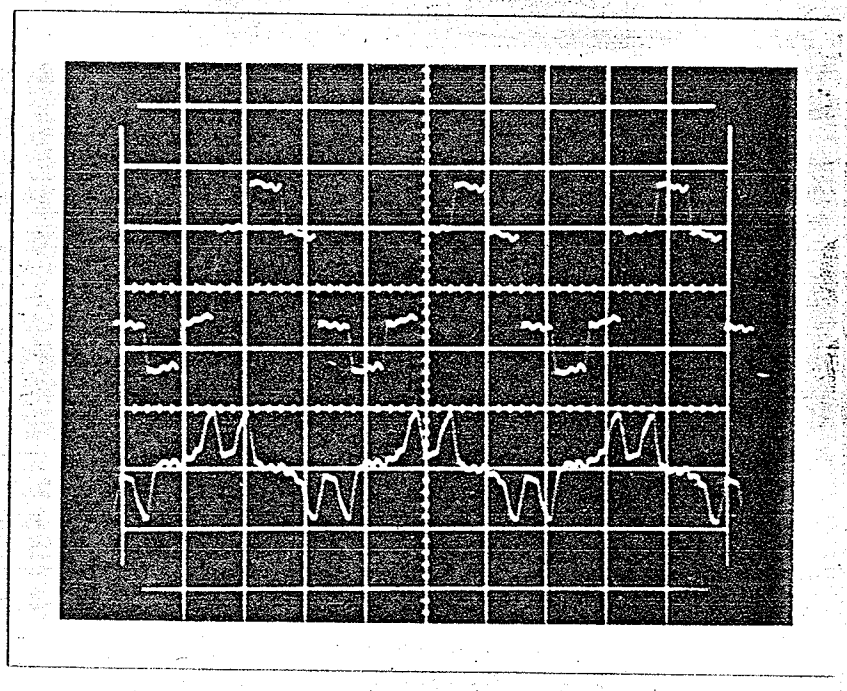

(b) Operation at 60 Hz. Horizontal scale: 5 ms/div.
Voltage (curve at top): Vert. scale: 200 V/div.
Current (curve at bottom): Vert. scale: 20 A/div.

Figure 4. Waveforms of line-to-line voltages and line currents in the stator windings with rotor ALASB in place.

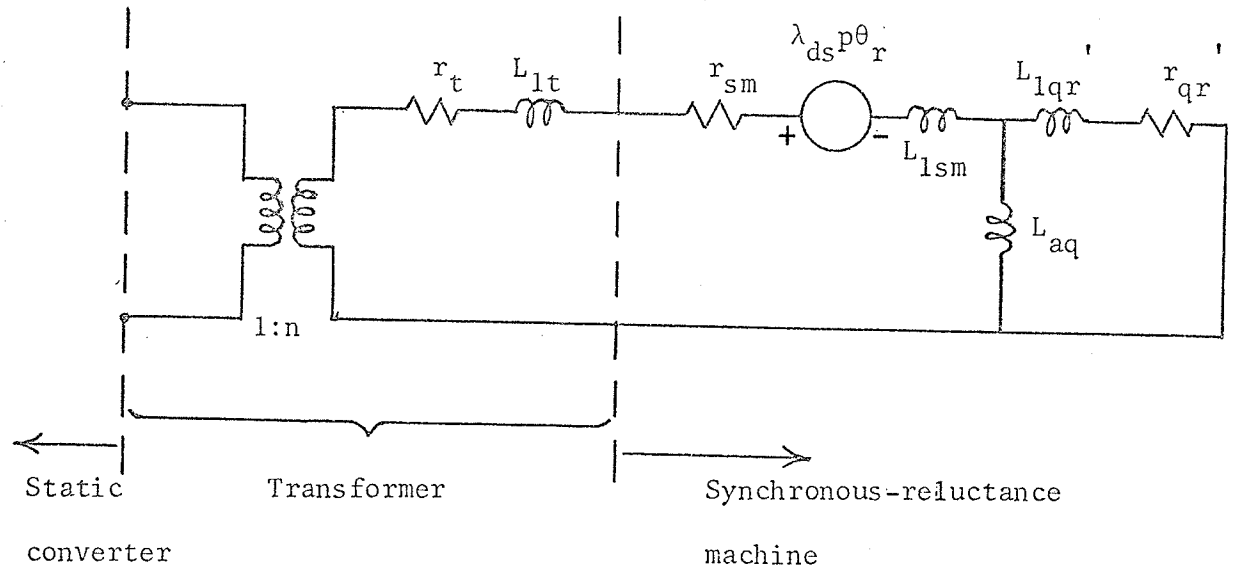

(a) Complete equivalent-circuit

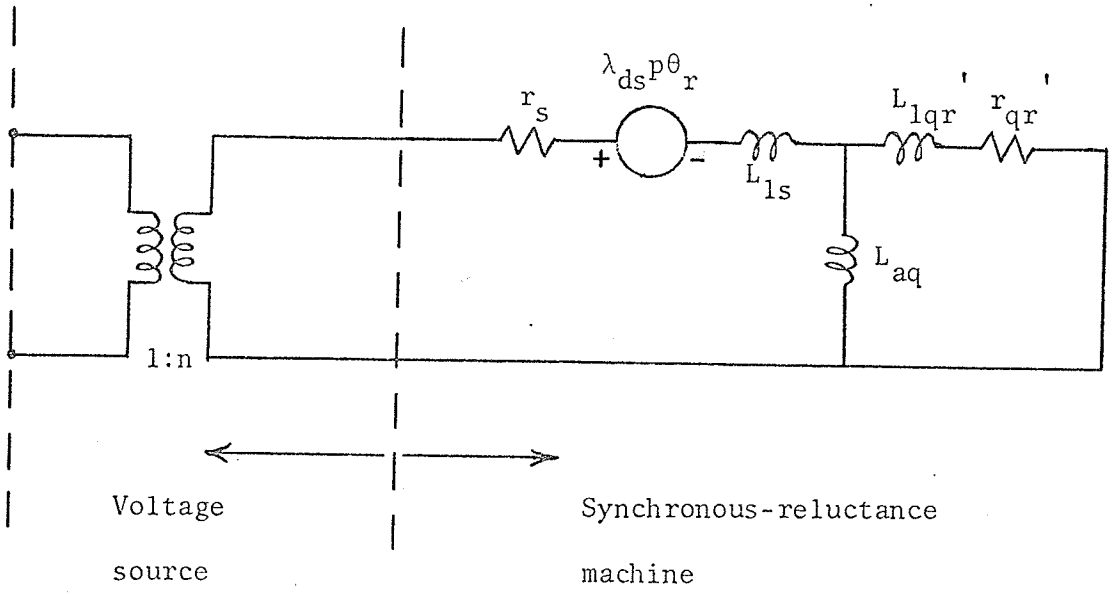

(b) Resultant equivalent-circuit

Figure 5. q-axis equivalent-circuit of system under test.

C. DETERMINATION OF MACHINE PARAMETERS

(a) Moments of inertia of rotors

The moments of inertia of the rotors were determined by the simple torsional pendulum method[10]. Each rotor was suspended from a steel wire by a bolt which was tightened into a centre hole drilled on one end of the rotor shaft. The period of simple harmonic torsional oscillations of each rotor was compared to the period of a standard cylinder of known mass and dimensions from which the moment of inertia of the cylinder was calculated. The moment of inertia of each rotor was computed using the equation:

$$J_r = \left(\frac{\tau_r}{\tau_{cy}}\right)^2 J_{cy} \qquad (65)$$

where $J_{cy} = \frac{1}{2} M R^2$.

(b) Stator leakage reactance (X_{ls})

The stator leakage reactance was found by locked-rotor-test on the machine with the squirrel-cage induction rotor in place. Neglecting the magnetizing impedance the total impedance $(r_s + r_r') + j(X_{ls} + X_{lr}')$ as seen from the stator terminals was measured. The stator leakage reactance X_{ls} was assumed to be equal to the equivalent rotor leakage reactance X_{lr}'.

(c) Stator resistance (r_s)

The stator resistances were found by d-c resistance bridge

measurements and were found to be equal.

(d) Direct-axis and quadrature-axis synchronous reactances (X_{ds} and X_{qs})

The d-axis and q-axis synchronous reactances for each machine setup were measured using d-c inductance bridge for various stator currents over the full working range. The variation of X_{qs} with stator currents was found to be very small and was considered constant. The value of X_{ds} varies considerably with stator currents. The value of X_{ds} used in the stability analysis is the value corresponding to the respective magnetic flux level. For low voltages the changes in magnetic fluxes are small and the value of X_{ds} used is the peak value (See Section (f) below).

(e) Direct-axis and quadrature-axis magnetizing reactances (X_{ad} and X_{aq})

The X_{ad} and X_{aq} values were calculated from the equations (37) and (38):-

$$X_{ad} = X_{ds} - X_{ls} \tag{66}$$

$$X_{aq} = X_{qs} - X_{ls} \tag{67}$$

(f) Direct-axis equivalent rotor resistance and equivalent rotor leakage reactance (r_{dr}' and X_{ldr}')

The d-axis subtransient impedance $\bar{Z}_d''$ for each machine

setup was measured by locked-rotor-test (Figure 6(a)). The rotor was locked at the position where minimum torque was sensed when the stator windings were energized. From the equivalent circuit as shown in Figure 7(a) both the equivalent rotor resistance r_{dr}' and equivalent rotor leakage reactance X_{ldr}' in the d-axis were calculated when $\bar{Z}_d''$, r_s and X_{ls} were known, X_{ad} being the peak value which occurs at low voltages.

(g) Quadrature-axis equivalent rotor resistance and equivalent rotor leakage reactance (r_{qr}' and X_{lqr}')

The q-axis subtransient impedance $\bar{Z}_q''$ for each machine setup was measured by locked-rotor-test (Figure 6(b)). The rotor was locked in the same position as in Section (f) above. Employing similar method as in (f) above, both the r_{qr}' and X_{lqr}' were calculated from the equivalent circuit as shown in Figure 7(b).

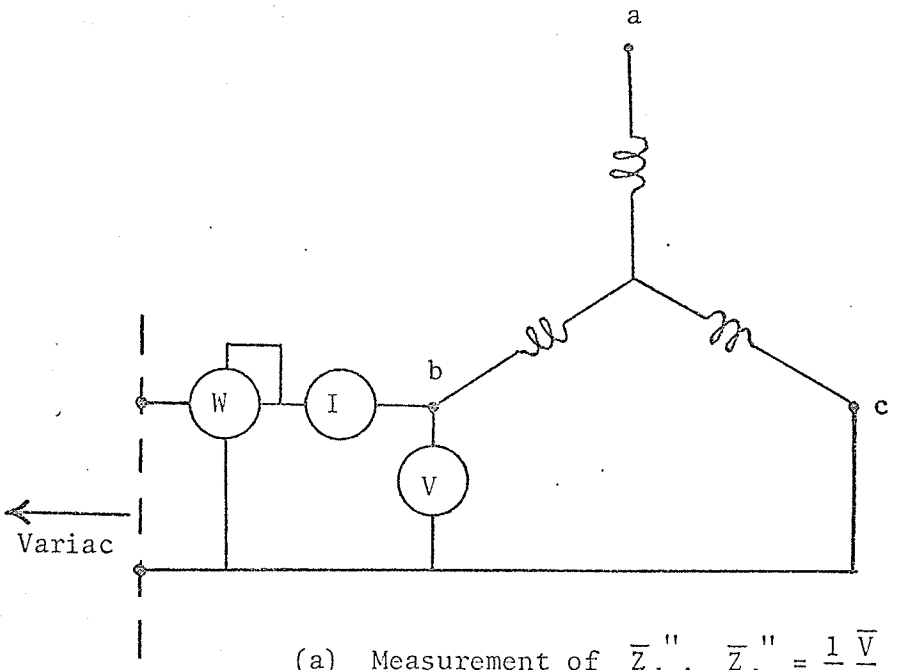

(a) Measurement of $\overline{Z}_d''$. $\overline{Z}_d'' = \frac{1}{2}\frac{\overline{V}}{\overline{I}}$

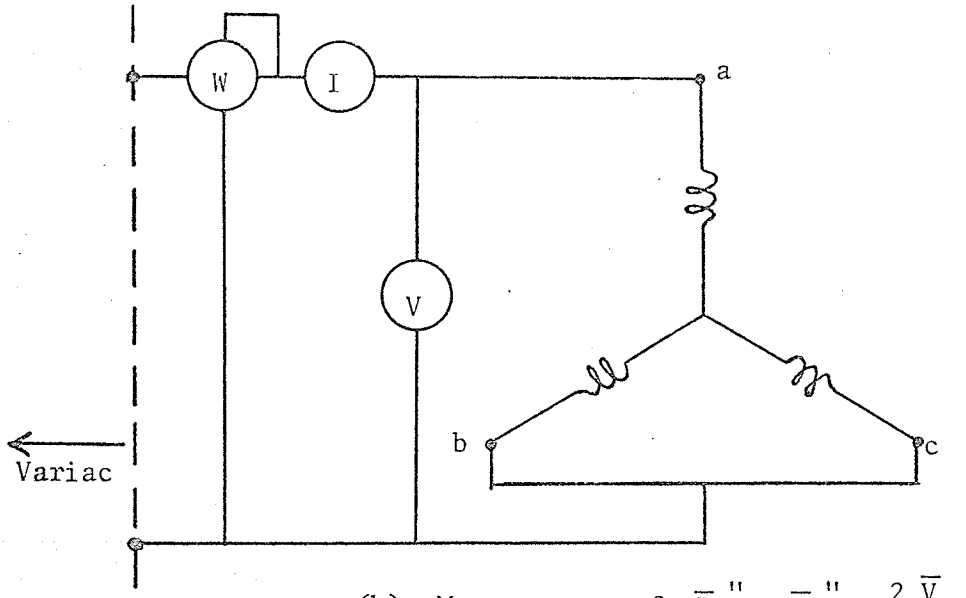

(b) Measurement of $\overline{Z}_q''$. $\overline{Z}_q'' = \frac{2}{3}\frac{\overline{V}}{\overline{I}}$

Figure 6. Measurement of the subtransient impedances.

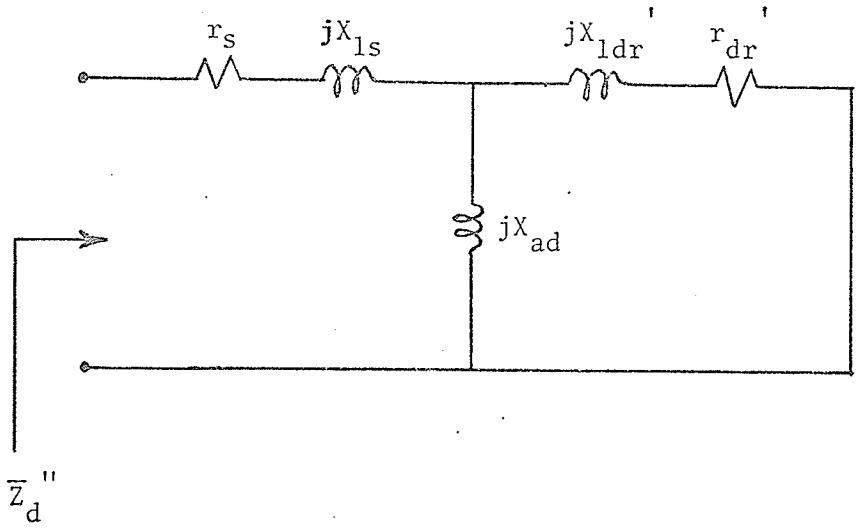

(a) d-axis

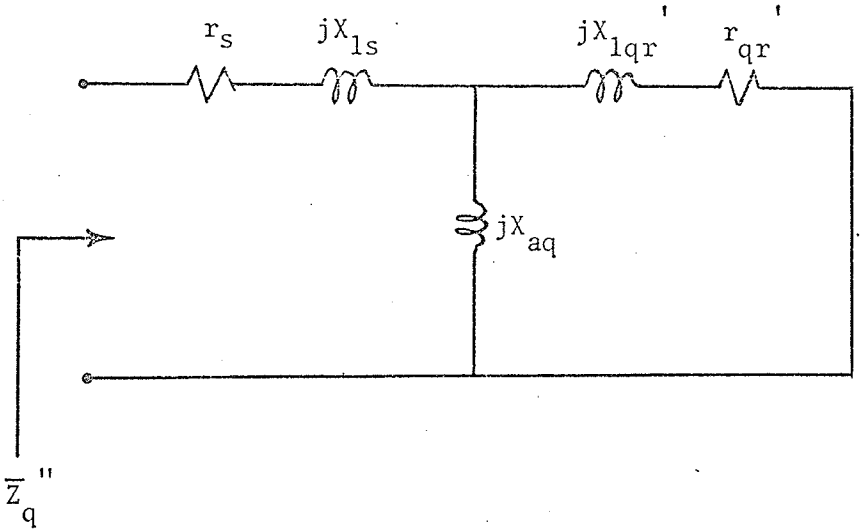

(b) q-axis

Figure 7. The d-axis and q-axis equivalent circuits for subtransient conditions.

CHAPTER VI

ANALYSIS OF THE RESULTS

Stability analysis was performed for each of the three machines at three magnetic flux levels, that is, at V_m = 0.866 p.u., V_m = 1.00 p.u., and V_m = 1.133 p.u. In the machine tests, a stroboscope was employed to check the stability of the machine. The stroboscope which was used to illuminate the rotor shaft was triggered from the line-to-neutral voltage of the stator winding and the position of a mark on the rotor shaft was observed. At the same time the waveforms of the stator currents were observed on an oscilloscope. The machine was first synchronized at f_r = 1.25 p.u., then the supply frequency was lowered very slowly until unstable operation of the machine was observed. The machine was regarded as unstable when the rotor was observed to undergo sustained oscillations about a mean position and when the amplitudes of the stator currents show noticeable sustained fluctuations. The machine was otherwise considered stable in the steady-state.

Figure 8, 9, and 10 show all the results from both the computer program and experiments. In one program the values of X_{ad} and X_{aq} are constant, and respectively correspond to the values at normal flux level. In another program each value of X_{ad} and X_{aq} has been corrected to the value measured at the particular flux level. Figure 8 also shows the effect of including a source impedance of (0.02 + j0.02) p.u. for the machine operated at normal flux level, that is, V_m = 1.00 p.u. Figure 9 also indicates the influence of rotor direct-axis resistance on the machine stability at normal flux level. Figure 10 also provides informations

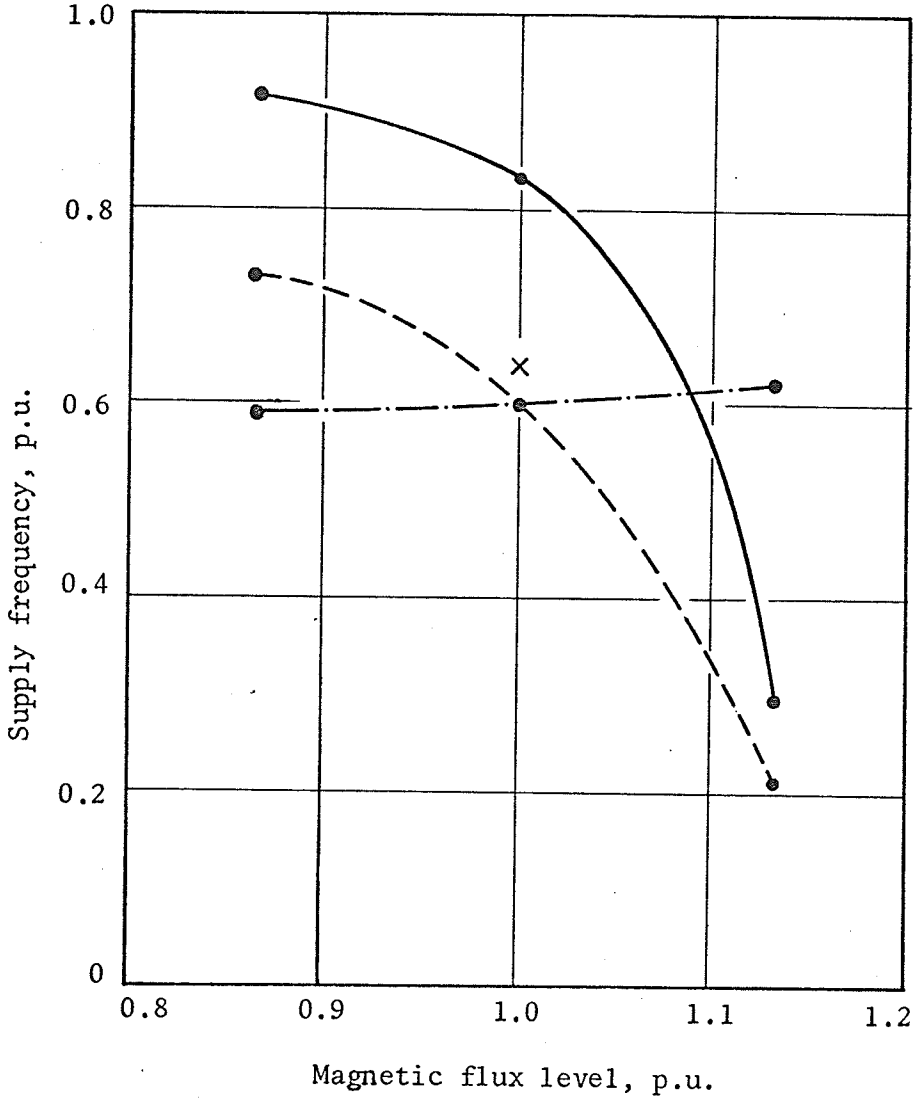

Figure 8. Stability boundaries for machine with rotor ALACN.

——— experimental boundary;

—·—·— theoretical boundary, X_{ad} and X_{aq} values constant for different V_m values;

– – – – theoretical boundary, corrected X_{ad} and X_{aq} values at different V_m values;

✕ theoretical boundary, a source impedance included.

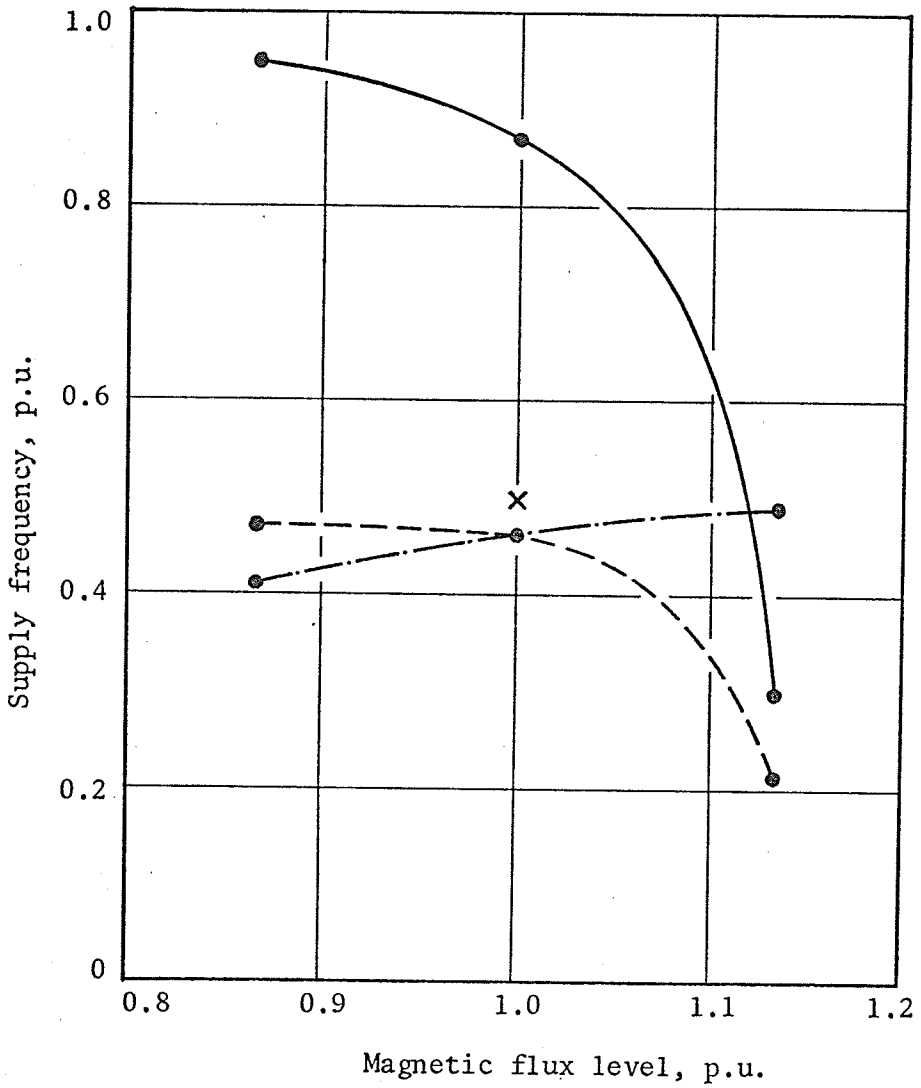

Figure 9. Stability boundaries for machine with rotor ALASN.

——— experimental boundary;

—·—·— theoretical boundary, X_{ad} and X_{aq} values constant for different V_m values;

– – – – theoretical boundary, corrected X_{ad} and X_{aq} values at different V_m values;

× theoretical boundary, r_{dr}' value increased by 5%.

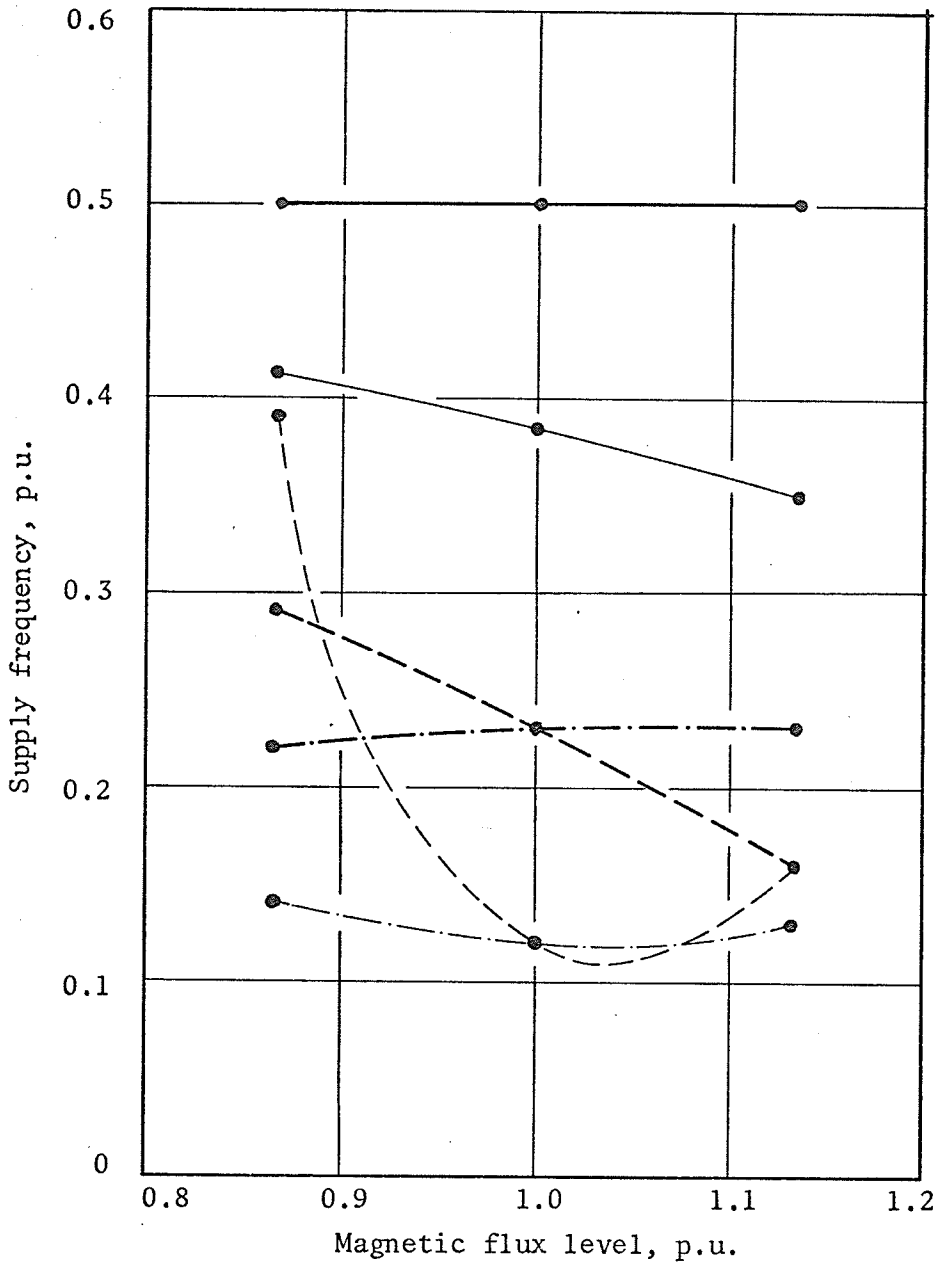

Figure 10. Stability boundaries for machine with rotor ALASB.

——— (thin) experimental boundary (H = 0.102);

—·—·— (thin) theoretical boundary (H = 0.102), X_{ad} and X_{aq} values constant for different V_m values;

– – – – (thin) theoretical boundary (H = 0.102), corrected X_{ad} and X_{aq} values at different V_m values;

——— (thick) experimental boundary (H = 0.548);

—·—·— (thick) theoretical boundary (H = 0.548), X_{ad} and X_{aq} values constant for different V_m values;

– – – – (thick) theoretical boundary (H = 0.548), corrected X_{ad} and X_{aq} values at different V_m values.

to show the influence of rotor inertia on the steady-state stability of the machine. In these three figures each machine is operated in the unstable mode below the critical frequencies indicated.

The experimental results disagree with the results obtained from the digital computer program in several aspects. From Figures 8, 9, and 10, in contrast with the experimental results, at no-load the stability boundaries predicted by the program, in which the X_{ad} and X_{aq} are constant, occur at higher frequencies with raised magnetic flux level. This is due to the fact that the values of X_{ad} and X_{aq} change with different flux levels, while the values of X_{ad} and X_{aq} in the computer program were instructed to stay constant at the values corresponding to normal flux level. The changes in the magnetic parameters were not taken into account in the program.

The tests on the machines show that each machine at no-load tends to be more stable at lower frequencies when the magnetic flux level is raised. This corresponds well with the digital computer prediction made by Lipo and Krause[8], and also with the results in this thesis, from the computer program in which each value of X_{ad} and X_{aq} has been corrected to the proper value at different magnetic flux levels. This can be realized as the effect of magnetic saturation at higher magnetic flux levels; saturation reduces the ratio of X_{ad}/X_{aq} and the machine becomes more stable. Therefore, it is invalid to predict machine steady-state stability by assuming the same values of X_{ad} and X_{aq} for different V_m values. At each flux level, the correct X_{ad} and X_{aq} values, and possibly also the correct X_{ldr}', X_{lqr}' and X_{ls} values, should be employed in the prediction of machine behavior.

By comparing the regions of instability for the machine with the rotor designated as ALASB for two different values of polar moment of inertia while all other parameters are unchanged, machine tests reveal that the machine becomes less stable at low frequencies when it has a higher polar moment of inertia. This increased region of instability is indicated for all the three magnetic flux levels. Prediction from the program does not show the shift of the region of stability in the same direction for $V_m = 0.866$ and for $V_m = 1.000$, but for $V_m = 1.133$ the stability boundaries are the same for both inertia values. The machine tests also show more or less the same stability boundary for all three flux levels with the higher value of inertia constant. Therefore, with a larger polar moment of inertia, the effect of changes in the magnetic flux level, on the size and location of the region of steady-state stability, is reduced as compared to the results obtained from tests on the machine with the lower moment of inertia wherein increasing the magnetic flux level improves the steady-state stability of the machine. However, we should not draw the conclusions that the machine with increased inertia should be less stable at low frequencies than with a lower inertia, and that the stability boundary tends to the same for different magnetic flux levels when the inertia is increased. We can only make such conclusions after many tests on different machines have confirmed that the same general trend is being followed. Tests on the machine with other rotors were not performed with increased inertia due to mechanical limitations.

The regions of instability at low operating frequencies, obtained from machine tests, are in all cases greater than those regions of

instability predicted by the digital computer program output with the correct X_{ad} and X_{aq} values for each flux level. These are due to one or more of the following:

1. The voltages supplied by the static converter are not sinusoidal while the prediction of machine behavior is based on the assumption that voltages applied to the stator terminals are sinusoidal. The approximately rectangular voltages from the static converter contain harmonics which tend to cause instability.
2. The 3-phase voltage source, the static converter, is in reality not a zero-impedance source. The output voltages vary, though slightly, with different loads. This means that there are interactions between the static converter and the reluctance machine to which the converter is delivering electrical power. The synchronous-reluctance machine is less stable when the voltage source interacts with the synchronous-reluctance machine. Yet in the theory developed in this thesis the voltage source is assumed to be independent of the machine to which it is supplying power. The effect of taking a source impedance into account is readily seen by examining the results shown in Figure 8. With the particular source impedance chosen the machine is less stable at low frequencies. However, there is no general method which enables us to measure the output impedance from the static converter, and this impedance varies with different loads.
3. The stator windings have different resistances and leakage

reactances, and the resistances and leakage reactances of the three step-up transformers are different. Hence the resultant resistance as well as the resultant leakage reactance of each stator phase is slightly different. The turns ratio of the three transformers are also not exactly equal. These give rise to both unbalance in the stator quantities and unbalance in the voltages supplied to the synchronous-reluctance machine. However, the values of these parameters fed into the computer program are the respective mean values, and balance is assumed in the program.

4. The measured machine parameter values are not accurate enough. Slight changes in any one of the parameters, for example, a 5% increase in the rotor direct-axis resistance, will cause fairly large shift in the steady-state stability boundary (see Figure 9). The resistances and dimensions of the machine are temperature variant. All these may cause disagreement in the relative size and location of the region of instability between values obtained from the computer program and from tests.

CHAPTER VII

CONCLUSIONS AND PROBLEMS FOR FUTURE STUDIES

The equations which describe the behavior of a synchronous-reluctance motor have been developed and these equations have been linearized employing the theory of small displacements. The Nyquist stability criterion has then been applied to predict the steady-state stability of the machine operating at variable frequency. Both machine tests and predictions obtained from the digital computer program applying the Nyquist stability criterion reveal regions of unstable operation at low operating frequencies when the machine is at no-load.

These regions of instability were found to be dependent upon the amplitude of the applied stator voltages, machine inertia, and machine parameters. The static converter is essentially a zero-impedance source and machine instability may occur at low frequencies due to insufficient damping within the machine.

In spite of the disagreements between the actual machine tests and the prediction applying the theory, this computer aided stability study employing the Nyquist stability criterion is able to predict the machine behavior during small disturbances from an operating point, regardless of the number of degree of the equations describing the machine behavior. This approach has the advantage over other techniques [See Chapter I, Section B] that the mathematical complexity in solving these high order equations [9] numerically is avoided while the modes of machine operation are readily found.

The future of the synchronous-reluctance machine appears to be in the adaptability to nonsinusoidal power supplies, such as those characteristic of the static converters used in variable-speed drives. Future studies should be made for machine behavior with different machine parameters, magnetic flux levels and machine inertia in order to correlate the machine behavior with nonsinusoidal power supplies to the machine behavior when it is subjected to sinusoidal power supplies. However, new methods should be developed for more accurate nonlinear analysis of machines operated from nonsinusoidal power supplies so as to establish criteria governing the design and improved performance-control of reluctance machines.

BIBLIOGRAPHY

1. P.J. Lawrenson and S.R. Bowes: "Stability of Reluctance Machines" Proc. IEE, Vol. 118, No. 2, pp. 356-369, Feb. 1971.
2. S.T. Bow, and J.E. Van Ness: "Use of Phase Space in Transient-Stability Studies", AIEE Trans. Pt. II, Applications & Industry, Vol. 77, pp. 187-191, Sept. 1958.
3. F. Fallside and J. Waddington: "Exact and Volterra Analysis of Synchronous Machine Stability", Int. J. Control, Vol. 11, No. 2, pp. 199-211, Feb. 1970.
4. R.G. Hoft: "Liapunov Stability Analysis of Reluctance Motors", IEEE Trans. Power Apparatus and Systems, Vol. PAS-87, No. 6, pp. 1485-1491, June 1968.
5. G.R. Slemon: "Magnetoelectric Devices", John Wiley and Sons, Inc., New York, 1966.
6. R.C. Dorf: "Modern Control Systems", Addison-Wesley Publishing Company, Massachusetts, 1967.
7. C. Concordia: "Synchronous Machines, Theory and Performance", John Wiley & Sons, Inc., New York, 1951.
8. T.A. Lipo and P.C. Krause: "Stability Analysis of a Reluctance-Synchronous Machine", IEEE Trans. Power Apparatus and Systems, Vol. PAS-86, No. 7, pp. 825-834, July 1967.
9. V.B. Honsinger: "Stability of Reluctance Motors", Presented at IEEE Power Engineering Society, Winter Meeting 1972. Paper No. T72 013-6, to be published in the Trans. Power Apparatus & Systems.
10. D.H. Fender: "General Physics and Sound", The English Universities Press Ltd., London, 1964.

11. B. Adkins: "The Generalized Theory of Electrical Machines", Chapman & Hall Ltd., 1962.

12. C.V. Jones: "The Unified Theory of Electrical Machines", Butterworths, London, 1967.

13. Harris, Lawrenson, and Stephenson: "Per-unit Systems with Special Reference to Electrical Machines", Cambridge at The University Press, 1970.

14. A.J.O. Cruickshank, A.F. Anderson and R.W. Menzies: "Theory and Performance of Reluctance Motors with Axially Laminated Antisotropic Rotors", Proc. IEE, Vol. 118, No. 7, pp. 887-894, July 1971.

15. J.F. Barrett: "The Use of Volterra Series to Find Region of Stability of a Non-linear Differential Equation", Int. J. Control, Vol. 1, First Series, pp. 209-216, March 1965.

16. J. Waddington and F. Fallside: "Analysis of Non-linear Differential Equations by the Volterra Series", Int. J. Control, Vol. 2, No. 1, pp. 1-15, Jan. 1966.

17. D.G. Schultz and J.E. Gibson: "The Variable Gradient Method of Generating Liapunov Functions", AIEE Trans. Applications and Industry, Vol. 81, Pt. II, pp. 203-210, Sept. 1962.

18. P.C. Krause and J.N. Towle: "Synchronous Machine Damping by Excitation Control with Direct and Quadrature Axis Field Windings", IEEE Trans. Power Apparatus and Systems, Vol. PAS-88, No. 8, pp. 1226-1274, Aug. 1969.

19. D.N. Ewart and F.P. deMello: "A Digital Computer Program for the Automatic Determination of Dynamic Stability Limits", IEEE Trans. Power Apparatus and Systems, Vol. PAS-86, No. 7, pp. 867-875, July 1967.

20. M.K. Khanijo and A.K. Mohanty: "Stability of Reluctance Synchronous Motor", IEEE Trans. Power Apparatus and Systems, Vol. PAS-87, No. 12, pp. 2009-2015, Dec. 1968.

21. T.A. Lipo and P.C. Krause: "Stability Analysis for Variable Frequency Operation of Synchronous Machines", IEEE Trans. Power Apparatus and Systems, Vol. PAS-87, No. 1, pp. 227-234, Jan. 1968.

22. P.C. Krause: "Method of Stabilizing a Reluctance Synchronous Machine", IEEE Trans. Power Apparatus and Systems, Vol. PAS-87, No. 3, pp. 641-649, March 1968.

23. P.C. Krause: "Method of Multiple Reference Frames Applied to the Analysis of Symmetrical Induction Machinery", IEEE Trans. Power Apparatus and Systems, Vol. PAS-87, No. 1, pp. 218-227, Jan. 1968.

24. P.J. Lawrenson and L.A. Agu: "Theory and Performance of Polyphase Reluctance Machines", Proc. IEE, Vol. 111, No. 8, pp. 1435-1445, Aug. 1964.

25. P.J. Lawrenson and J.M. Stephenson: "Average Asynchronous Torque of Synchronous Machines, With Particular Reference to Reluctance Machines", Proc. IEE, Vol. 116, No. 6, pp. 1049-1951, June 1969.

26. H.E. Jordan: "Analysis of Induction Machines in Dynamic Systems", IEEE Trans. Power Apparatus and Systems, Vol. PAS-84, No. 11, pp. 1080-1085, Nov. 1965.

27. M. Riaz: "Analogue Computer Representations of Synchronous Generators in Voltage-Regulation Studies", AIEE Trans., Pt. III Power Apparatus and Systems, Vol. 75, pp. 1178-1184, Dec. 1956.

28. T.H. Barton and J.C. Dunfield: "Polyphase to Two-Axis Transformation for Real Windings", IEEE Trans. Power Apparatus and Systems, Vol.

PAS-87, No. 5, pp. 1342-1354, May 1968.

29. J.K. Lubbock and V.S. Bansal" "Multidimensional Laplace transforms for solution of nonlinear equations", Proc. IEE, Vol. 116, No. 12, pp. 2075-2082, Dec. 1969.

30. V.B. Honsinger: "Steady state performance of reluctance Machines", IEEE Trans. Power Apparatus and Systems, Vol. Pas-90, pp. 305-311, Jan./Feb. 1971.

31. V.B. Honsinger: "The Inductances L_d and L_q of Reluctance Machines", IEEE Trans. Power Apparatus and Systems, Vol. PAS-90, pp. 298-304, Jan./Feb. 1971.

32. A.J. Ellison: "Generalized Electric Machines", George G. Harrap & Co. Ltd., London, 1967.

33. G. Kron: "Equivalent Circuits of Electric Machinery", John Wiley & Sons, Inc., New York, 1951.

34. D.W. Olive : "Digital Simulation of Synchronous Machine Transients", IEEE Trans. Power Apparatus and Systems, Vol. PAS-87, No. 8, pp. 1669-1675, Aug. 1968.

35. R.W. Menzies: "Theory and Operation of Reluctance Motors with Magnetically Anisotropic Rotors; Part I. Analysis", IEEE Trans. Power Apparatus and Systems, Vol. PAS-91, No. 1, pp. 35-41, Jan./ Feb., 1972

36. R.W. Menzies, R.M. Mathur, and H.W. Lee: "Theory and Operation of Reluctance Motors with Magnetically Anisotropic Rotors; Part II. Synchronous Performance", IEEE Trans. Power Apparatus and Systems, Vol. PAS-91, No.1, pp. 42-45, Jan./Feb., 1972.

APPENDIX A

LIST OF SYMBOLS

SYMBOLS:

f = frequency (Hz); or variables used in equations (18) through (20).

f_r = steady-state frequency, defined by eqn. (40) (Hz).

$F(j\nu)$ = function, defined in eqn. (63).

$G(j\nu)$ = function, defined in Appendix C.

H = inertial constant of machine (s).

i = instantaneous current (A).

I = current, either peak or rms value (A).

j = imaginary part of a quantity.

J = polar moment of inertia ($kg \cdot m^2$).

L = inductance (H).

M = mass of standard cylinder (kg).

N = number of turns in the winding.

n = turns ratio of transformer.

p = operator $\frac{d}{dt}$.

P = number of pole pairs.

r = phase-winding resistance (Ω).

R = radius of standard cyliner (m).

t = time (s).

v = instantaneous voltage (V).

V = terminal voltage, amplitude or rms value (V).

V_m = terminal voltage at base frequency (V).

s = Laplace variable.

W = real power (W).

X = reactance (Ω).

Z = impedance (Ω).

Z'' = subtransient impedance (Ω).

Δ = small changes in a variable.

δ = angle by which the direct axis leads the stator potential in electrical radians.

θ_r = instantaneous position of rotor, in electrical radians.

θ_{rm} = instantaneous position of rotor, in mechanical radians.

λ = magnetic flux linkage in volt-seconds.

π = numerical constant, equals 3.14159....

τ = period of oscillations, in measurement of polar moment of inertia (s).

Σ = summation of (Einstein's notation).

T = torque (N·m).

ν = frequency of oscillations of rotor (rad/s).

ω = angular frequency (rad/s).

Ω = ohms.

∞ = mathematical notation, equals infinity.

SUPERSCRIPTS:

$-$ = phasor quantities.

$'$ = prime rotor quantities, referred to stator winding side.

SUBSCRIPTS:

a, b, and c = stator phase quantities.

d, q = direct and quadrature axes quantities.

cy = standard cylinder quantities.

r, s = rotor and stator quantities.

k = damper winding quantities.

l = leakage quantities.

0 = steady-state quantities.

e = electrical quantities.

L = mechanical load quantities.

m = actual machine quantities.

~ = per unit quantities.

t = transformer quantities.

APPENDIX B

SOLVING FOR Δi_{qs} AND Δi_{ds} IN EQN. (55) AND FOR ΔT_e IN EQN. (57)

In this appendix all quantities, except p and ω_e, are in per unit values. Equations (55) can be written as:

$$\left[-V \sin \delta_0 + \frac{P}{\omega_e} X_{ds}\, i_{ds0}\right]\Delta\delta = \left[r_s + \frac{p}{\omega_e} X_{qs} - \frac{(\frac{p}{\omega_e})^2 X_{aq}^2}{r_{qr}' + \frac{p}{\omega_e} X_{qr}'}\right]\Delta i_{qs} + \left[X_{ds}\, f_r - \frac{\frac{p}{\omega_e} f_r X_{ad}^2}{r_{dr}' + \frac{p}{\omega_e} X_{dr}'}\right]\Delta i_{ds} \qquad (68)$$

$$\left[V \cos \delta_0 + \frac{P}{\omega_e} X_{qs}\, i_{qs0}\right]\Delta\delta = \left[-X_{qs}\, f_r + \frac{\frac{p}{\omega_e} f_r X_{aq}^2}{r_{qr}' + \frac{p}{\omega_e} X_{qr}'}\right]\Delta i_{qs} + \left[r_s + \frac{p}{\omega_e} X_{ds} - \frac{(\frac{p}{\omega_e})^2 X_{ad}^2}{r_{dr}' + \frac{p}{\omega_e} X_{dr}'}\right]\Delta i_{ds} \qquad (69)$$

By eliminating Δi_{qs} in (68) and (69) we can solve for Δi_{ds}:

$$\Delta i_{ds} = \left\{r_{kd}(E_1 + E_5) + \left[r_{kd}(E_2 + E_6) + X_{kd}(E_1 + E_5)\right]D + \left[r_{kd}(E_3 + E_7) + X_{kd}(E_2 + E_6)\right]D^2 + \left[r_{kd}\, E_4 + X_{kd}(E_3 + E_7)\right]D^3 + X_{kd}\, E_4\, D^4\right\}\Delta\delta \Big/ \left\{(E_{10} + E_{15}) + (E_{11} + E_{16})D + (E_{12} + E_{17})D^2 + E_{13}\, D^3 + E_{14}\, D^4\right\} \qquad (70)$$

By eliminating Δi_{ds} from equations (68) and (69) we can solve for Δi_{qs} and the following may be obtained:

$$\Delta i_{qs} = \Big\{ r_{kq}(B_1 + B_4) + \Big[r_{kq}(B_2 + B_5) + X_{kq}(B_1 + B_4) \Big] D + \Big[r_{kq}(B_3 + B_6) + X_{kq}(B_2 + B_5) \Big] D^2 + \Big[r_{kq} B_7 + X_{kq}(B_3 + B_6) \Big] D^3 + X_{kq} B_7 D^4 \Big\} \Delta\delta \Big/ \Big\{ (B_{12} + B_{17}) + (B_{10} + B_{13}) D + (B_{11} + B_{14}) D^2 + B_{15} D^3 + B_{16} D^4 \Big\} \qquad (71)$$

In obtaining equations (70) and (71) we use the following symbols:

$$D = \frac{p}{\omega_e}$$

$$r_{kd} = r_{dr}'$$

$$r_{kq} = r_{qr}'$$

$$X_{kd} = X_{dr}'$$

$$X_{kq} = X_{qr}'$$

$$R_D = r_{dr}' X_{ds} + r_s X_{dr}'$$

$$R_Q = r_{qr}' X_{qs} + r_s X_{qr}'$$

$$X_D = X_{ds}\, X_{dr}' - X_{ad}^2$$

$$X_Q = X_{qs}\, X_{qr}' - X_{aq}^2$$

$$B_1 = f_r\, r_{kd}\, X_{ds}\, V \cos \delta_0$$

$$B_2 = f_r\, X_D\, V \cos \delta_0 + f_r\, r_{kd}\, X_{ds}\, X_{qs}\, i_{qs0}$$

$$B_3 = f_r\, X_D\, X_{qs}\, i_{qs0}$$

$$B_4 = r_s\, r_{kd}\, V \sin \delta_0$$

$$B_5 = R_D\, V \sin \delta_0 + r_s\, r_{kd}\, X_{ds}\, i_{ds0}$$

$$B_6 = X_D\, V \sin \delta_0 + R_D\, X_{ds}\, i_{ds0}$$

$$B_7 = X_D\, X_{ds}\, i_{ds0}$$

$$B_{10} = -f_r^2\, r_{kq}\, X_{qs}\, X_D - f_r^2\, r_{kd}\, X_{ds}\, X_Q$$

$$B_{11} = -f_r^2\, X_D\, X_Q$$

$$B_{12} = -r_s^2\, r_{kd}\, r_{kq}$$

$$B_{13} = -(r_s\, r_{kq}\, R_D + r_s\, r_{kd}\, R_Q)$$

$$B_{14} = -(r_s\, r_{kq}\, X_D + R_D\, R_Q + r_s\, r_{kd}\, X_Q)$$

$$B_{15} = -(R_Q\, X_D + R_D\, X_Q)$$

$$B_{16} = -\, X_D\, X_Q$$

$$B_{17} = -\, f_r^2\, r_{kd}\, r_{kq}\, X_{ds}\, X_{qs}$$

$$E_1 = r_s\, r_{kq}\, V \cos \delta_0$$

$$E_2 = R_Q\, V \cos \delta_0 + r_s\, r_{kq}\, X_{qs}\, i_{qs0}$$

$$E_3 = X_Q\, V \cos \delta_0 + X_{qs}\, R_Q\, i_{qs0}$$

$$E_4 = X_{qs}\, X_Q\, i_{qs0}$$

$$E_5 = - f_r\, r_{kq}\, X_{qs}\, V \sin \delta_0$$

$$E_6 = - f_r\, X_Q\, V \sin \delta_0 - f_r\, r_{kq}\, X_{qs}\, X_{ds}\, i_{ds0}$$

$$E_7 = - f_r\, X_{ds}\, X_Q\, i_{ds0}$$

$$E_{10} = r_s^2\, r_{kd}\, r_{kq}$$

$$E_{11} = r_s(r_{kd}\, R_Q + r_{kq}\, R_D)$$

$$E_{12} = r_s(r_{kd}\, X_Q + r_{kq}\, X_D) + R_D\, R_Q$$

$$E_{13} = R_D\, X_Q + R_Q\, X_D$$

$$E_{14} = X_D\, X_Q$$

$$E_{15} = f_r^2\, r_{kd}\, r_{kq}\, X_{ds}\, X_{qs}$$

$$E_{16} = f_r^2\, r_{kd}\, X_{ds}\, X_Q + f_r^2\, r_{kq}\, X_{qs}\, X_D$$

$$E_{17} = f_r^2\, X_D\, X_Q$$

writing Δi_{ds} and Δi_{qs} in (70) and (71) as

$$\Delta i_{ds} = A_1(p)\, \Delta\delta \tag{72}$$

and

$$\Delta i_{qs} = A_2(p)\, \Delta\delta \tag{73}$$

and after substituting these values of Δi_{ds} and Δi_{qs} into (57) we obtain the following:

$$\Delta T_e = \frac{3}{\omega_e} \left\{ \left[(X_{ds} - X_{qs}) + \frac{(\frac{p}{\omega_e}) X_{aq}^2}{r_{qr}' + \frac{p}{\omega_e} X_{qr}'} \right] i_{ds0} A_2(p) \Delta\delta \right.$$

$$+ \left[(X_{ds} - X_{qs}) - \frac{\frac{p}{\omega_e} X_{ad}^2}{r_{dr}' + \frac{p}{\omega_e} X_{dr}'} \right] i_{qs0} A_1(p) \Delta\delta$$

$$= \frac{3}{\omega_e} \left\{ \left[(X_{ds} - X_{qs}) + \frac{\frac{p}{\omega_e} X_{aq}^2}{r_{qr}' + \frac{p}{\omega_e} X_{qr}'} \right] i_{ds0} A_2(p) \right.$$

$$\left. + \left[(X_{ds} - X_{qs}) - \frac{\frac{p}{\omega_e} X_{ad}^2}{r_{dr}' + \frac{p}{\omega_e} X_{dr}'} \right] i_{qs0} A_1(p) \right\}$$

$$x \quad \Delta\delta \qquad (74)$$

With $G(p) = \frac{3}{\omega_e} \left\{ \left[(X_{ds} - X_{qs}) + \frac{\frac{p}{\omega_e} X_{aq}^2}{r_{qr}' + \frac{p}{\omega_e} X_{qr}'} \right] i_{ds0} A_2(p) \right.$

$$\left. + \left[(X_{ds} - X_{qs}) - \frac{\frac{p}{\omega_e} X_{ad}^2}{r_{dr}' + \frac{p}{\omega_e} X_{dr}'} \right] i_{qs0} A_1(p) \right\}$$

equation (74) becomes (58):

$$\Delta T_e = G(p) \Delta\delta \qquad (58)$$

APPENDIX C

EXPRESSION FOR $G(j\nu)$

In this appendix all quantities are expressed in per unit values. The following terms are used for convenience to express $G(j\nu)$:

$$s = \nu/\omega_e$$

$$X_D = X_{ds} X_{dr}' - X_{ad}^2$$

$$X_Q = X_{qs} X_{qr}' - X_{aq}^2$$

$$R_D = r_{dr}' X_{ds} + r_s X_{dr}'$$

$$R_Q = r_{qr}' X_{qs} + r_s X_{qr}'$$

$$R_{VS} = r_{qr}' V \sin \delta_0 - s^2 X_{ds} X_{qr}' i_{ds0}$$

$$R_{VC} = r_{qr}' V \cos \delta_0 - s^2 X_{qs} X_{qr}' i_{qs0}$$

$$X_{VS} = X_{qr}' V \sin \delta_0 + X_{ds} r_{qr}' i_{ds0}$$

$$X_{VC} = X_{qr}' V \cos \delta_0 + X_{qs} r_{qr}' i_{qs0}$$

$$N_{10} = - \left[r_s r_{dr}' - s^2 X_D \right] R_{VS}$$

$$N_{11} = f_r r_{dr}' X_{ds} R_{VC}$$

$$N_{12} = s^2 R_D X_{VS}$$

$$N_{13} = s^2 f_r X_D X_{VC}$$

$$P_{10} = - s \left[r_s r_{dr}' - s^2 X_D \right] X_{VS}$$

$$P_{11} = s\, f_r\, r_{dr}'\, X_{ds}\, X_{VC}$$

$$P_{12} = s\, R_D\, R_{VS}$$

$$P_{13} = s\, f_r\, X_D\, R_{VC}$$

$$P_{15} = (r_{dr}'\, V \cos \delta_0 - s^2\, X_{qs}\, X_{dr}'\, i_{qs0})\, (r_s\, r_{qr}' - s^2\, X_Q)$$

$$P_{16} = f_r\, r_{qr}'\, X_{qs}\, (r_{dr}'\, V \sin \delta_0 - s^2\, X_{ds}\, X_{dr}'\, i_{ds0})$$

$$P_{17} = s^2\, R_Q\, (X_{dr}'\, V \cos \delta_0 + X_{qs}\, r_{dr}'\, i_{qs0})$$

$$P_{18} = s^2\, f_r\, X_Q\, (X_{dr}'\, V \sin \delta_0 + X_{ds}\, r_{dr}'\, i_{ds0})$$

$$S_{10} = s\, R_Q\, (r_{dr}'\, V \cos \delta_0 - s^2\, X_{qs}\, X_{dr}'\, i_{qs0})$$

$$S_{11} = s\, f_r\, X_Q\, (r_{dr}'\, V \sin \delta_0 - s^2\, X_{ds}\, X_{dr}'\, i_{ds0})$$

$$S_{12} = s\, (r_s\, r_{qr}' - s^2\, X_Q)\, (X_{dr}'\, V \cos \delta_0 + X_{qs}\, r_{dr}'\, i_{qs0})$$

$$S_{13} = s\, f_r\, r_{qr}'\, X_{qs}\, (X_{dr}'\, V \sin \delta_0 + X_{ds}\, r_{dr}'\, i_{ds0})$$

$$H_{10} = r_s^2\, r_{qr}'\, r_{dr}' + f_r^2\, r_{qr}'\, r_{dr}'\, X_{ds}\, X_{qs} - s^2\, r_s\, r_{dr}'\, X_Q$$

$$H_{12} = s^2\, (f_r^2 - s^2)\, X_Q\, X_D$$

$$K_{10} = s\, r_s\, r_{dr}'\, R_Q + s\, r_s\, r_{qr}'\, R_D$$

$$K_{11} = s\, f_r^2\, r_{dr}'\, X_{ds}\, X_Q + s\, f_r^2\, r_{qr}'\, X_{qs}\, X_D$$

$$A_1 = (X_{ds} - X_{qs})\, r_{qr}'\, i_{ds0}$$

$$A_2 = s \left[X_{qr}'\, (X_{ds} - X_{qs}) + X_{aq}^2 \right] i_{ds0}$$

$$A_3 = N_{10} - N_{11} + N_{12} + N_{13}$$

$$A_4 = P_{10} - P_{11} - P_{12} - P_{13}$$

$$A_5 = (X_{ds} - X_{qs})\, r_{dr}'\, i_{qs0}$$

$$A_6 = s\left[X_{dr}'\,(X_{ds} - X_{qs}) - X_{ad}^2\right] i_{qs0}$$

$$A_7 = P_{15} - P_{16} - P_{17} + P_{18}$$

$$A_8 = S_{10} - S_{11} + S_{12} - S_{13}$$

$$A_9 = H_{10} - s^2\, r_s\, r_{qr}'\, X_D - s^2\, R_Q\, R_D - H_{12}$$

$$A_{10} = K_{10} + K_{11} - s^3\, R_D\, X_Q - s^3\, R_Q\, X_D$$

$$A_{11} = r_{qr}'$$

$$A_{12} = s\, X_{qr}'$$

$$A_{13} = r_{dr}'$$

$$A_{14} = s\, X_{dr}'$$

The expression for $G(j\nu)$ can be written as

$$G(j\nu) = \frac{(A_1 + j\,A_2)(A_3 + j\,A_4)}{(A_9 + j\,A_{10})(A_{11} + j\,A_{12})} + \frac{(A_5 + j\,A_6)(A_7 + j\,A_8)}{(A_9 + j\,A_{10})(A_{13} + j\,A_{14})} \quad (75)$$

By employing the conventional rules of complex numbers, the expression for $G(j\nu)$ can be written as:

$$G(j\nu) = a(\nu) + j\,b(\nu) \quad (76)$$

But in the calculation of $F(j\nu)$, it is not necessary to convert the expression for $G(j\nu)$ to its simpler form as in (76). The form as defined in (75) is used in the computer program. Note that the term $\frac{3}{\omega_e}$ in the electric torque expression vanishes when all the other quantities in that expression are expressed in per unit quantities. Hence, $G(j\nu)$ does not contain the term $\frac{3}{\omega_e}$.

The transfer function $G(j\nu)$ in Laplace transform notation for the machine ALACN operated at $V_m = 1.0$ p.u. and $f_r = 0.96$ p.u. (See Chapter IV, Section A) is

$$G(s) \approx \{(-1.6024)(251.0 + 884.4s)(9.97 + 74.30s + 175.01s^2 + 167.51s^3 + 125.47s^4)\} / \{2.00 + 14.43s + 32.92s^2 + 28.61s^3 + 14.84s^4\}$$

or $$G(s) \approx \{-1.815 \times 10^{-3}(s + 0.284)(s + 0.335)(s + 0.277)(s + 0.361 + j0.854)(s + 0.361 - j0.854)\} / \{(s + 0.373)(s + 0.282)(s + 0.639 + j0.926)(s + 0.639 - j0.926)\}$$

where s is the Laplace variable.

APPENDIX D

DIGITAL COMPUTER PROGRAM USED TO GENERATE DATA POINTS FOR THE PLOT OF $F(j\nu)$

```
C
C
C       STEADY-STATE STABILITY STUDIES OF A SYNCHRONOUS-RELUCTANCE MACHINE,
C       EMPLOYING NYQUIST STABILITY CRITERION
C
C
C       IDSO --- STEADY-STATE D-AXIS STATOR CURRENT IN PER UNITS
C       IQSO --- STEADY-STATE Q-AXIS STATOR CURRENT IN PER UNITS
C       WE --- BASE FREQUENCY IN RADIANS PER SECOND
C       RAVL --- RATED STATOR LINE VOLTAGE IN VOLTS RMS
C       RAIP --- RATED STATOR PHASE CURRENTS IN AMPERES RMS
C       RS --- STATOR RESISTANCE PER PHASE IN OHMS
C       XLS --- STATOR LEAKAGE REACTANCE PER PHASE IN OHMS
C       XAD, XAQ --- D-AXIS AND Q-AXIS MAGNETIZING REACTANCES IN OHMS
C       XLKD, XLKQ --- D-AXIS AND Q-AXIS LEAKAGE REACTANCES OF DAMPER CIRCUITS I
C       OHMS
C       RKD, RKQ --- D-AXIS AND Q-AXIS DAMPER WINDING RESISTANCES IN OHMS
C       HC --- INERTIA CONSTANT OF ROTOR (PER UNIT MOMENT OF INERTIA DIVIDED BY
C       TWO TIMES BASE FREQUENCY)
C       ZN --- BASE IMPEDANCE OF STATOR CIRCUIT
C       XDS, XQS --- D-AXIS AND Q-AXIS SYNCHRONOUS REACTANCES OF STATOR IN PER
C       UNITS
C       XKD, XKQ --- D-AXIS AND Q-AXIS REACTANCES OF DAMPER CIRCUIT IN PER UNITS
C       VMM --- MAGNETIC FLUX LEVEL, EQUALS PER UNIT STATOR VOLTAGE AT BASE
C       FREQUENCY
C       VM --- PER UNIT STATOR VOLTAGE AT A PARTICULAR FREQUENCY
C       TEO --- STEADY-STATE ELECTRIC TORQUE IN PER UNITS
C       FR --- PER UNIT FREQUENCY OF VOLTAGE SUPPLY
C       WP --- FREQUENCY OF ROTOR OSCILLATIONS IN RADIANS PER SECOND
C       V --- PER UNIT FREQUENCY OF ROTOR OSCILLATION
C       GJV --- TRANSFER FUNCTION FROM CHANGES IN DELTO TO CHANGES IN ELECTRIC
C       TORQUE
C       FGV --- OPEN-LOOP TRANSFER FUNCTION OF SYSTEM AS DERIVED FROM THEORY
C
C
      REAL L,M,N,K
      REAL IDSO, IQSO
      REAL N10,N11,N12,N13,K10,K11,K12,N1
      COMPLEX CMPLX
      COMPLEX CN1,CN2,CN3,CN4,CD1,CD2,CD3,GJV,FGV
C
C
C     DATA
C
C *** BASE QUANTITIES
C
      RAVL=220.0
      RAIP=8.6
      ZN=RAVL/SQRT(3.00)/RAIP
      WE=377.0
C
C     STATOR QUANTITIES
C
      VMM=0.366
      RS=0.8063
      XLS=0.8515
C
C
```

```
C       ROTOR ALASB
C
         HC=0.102
        XAD=13.6
        XAQ=3.2
        XLKD=0.5724
        XLKQ=1.0254
        RKD=0.8468
        RKQ=1.0559
C
C       ROTOR ALASB
C
C       DATA END
C
C
C *** NORMALIZATION --- CHANGE ALL QUANTITIES TO PER UNIT QUANTITIES
C
        XAQ=XAQ/ZN
        XLKD=XLKD/ZN
        XLKQ=XLKQ/ZN
        RKD=RKD/ZN
        RKQ=RKQ/ZN
 2      RS=RS/ZN
        XLS=XLS/ZN
        XAD=XAD/ZN
C
C       NORMALIZATION ENDS
C
C       PRINT OUT MACHINE DATA
C
        WRITE (6, 3)
 3      FORMAT (////,'       ROTOR ALASB'//G10.5)
        WRITE (6, 8) ZN,RS,XLS,XAD,XAQ,XLKD,XLKQ,RKD,RKQ
 8      FORMAT (////'      ZN =',F8.4,'     RS =',F7.4,'     XLS =',F7.4,'
     1 XAD =',F7.4,'     XAQ =',F7.4/'      XLKD =',F7.4,'     XLKQ =',F7.4
     2,'     RKD =',F7.4,'     RKQ =',F7.4////)
        WRITE (6, 6)
 6      FORMAT(1H1)
C
C
        XDS=XAD+XLS
        XQS=XAQ+XLS
        XKD=XLKD+XAD
        XKQ=XLKQ+XAQ
        A1=RS**2
        A3=XDS-XQS
        A4=XDS+XQS
        XD=XDS*XKD-XAD**2
        RD=RKD*XDS+RS*XKD
        XQ=XQS*XKQ-XAQ**2
        RQ=RKQ*XQS+RS*XKQ
C
C       VMM LOOP
C
C       FR LOOP
        FR=0.030
C
30      VM=FR*VMM
```

```
      A2=FR**2*XDS*XQS
      A5=A1+A2
      N1=A5**2
      D1=VM**2*A3
      REES=N1/D1
      B=A2-A1
      C=FR*RS*A4
      CK=FR*RS*A3
C
C     TEO LOOP
C
      TEO=0.00
C
C
C     CALCULATION OF STEADY-STATE ELECTRIC LOAD ANGLE DELTO
C
40    AA=TEO*REES*2.000
      A6=AA+CK
      BAB=B*B+C*C-A6*A6
      IF (BAB .LT. 0.0) GO TO 500
      D2=SQRT (BAB)
      DELTO= -0.50*ATAN (A6/D2) + 0.50 *ATAN (C/B)
C
C
C     CALCULATION OF STEADY-STATE STATOR CURRENTS  IDSO AND IQSO
C
      VS=VM*SIN(DELTO)
      VC=VM*COS(DELTO)
      IDSO=(RS*VS+FR*XQS*VC)/A5
      IQSO=(RS*VC-FR*XDS*VS)/A5
C
C     PRINT OUT VMM, FR, TEO , DELTO, IDSO, AND IQSO.
C
70    WRITE (6, 75) VMM,FR,TEO,DELTO,IDSO,IQSO
75    FORMAT (/'  VMM =',F7.4,'      FR =',F7.4,'      TEO =',F7.4,'      D
     1ELTO =',F7.4,'      IDSO =',F7.4,'      IQSO =',F7.4)
C
C     CALCULATE GJV
C
90    DO 101 I=2,24
      UP=(I**3+0.00)/100.00
      V=UP/WE
      VV=V**2
      L=A3*RKQ*IDSO
      M=V*(XKQ*A3+XAQ**2)*IDSO
      XX1=RS*RKD-VV*XD
      XX2=RS*RKQ-VV*XQ
      RVS=RKQ*VS-VV*XDS*XKQ*IDSO
      RVC=RKQ*VC-VV*XQS*XKQ*IQSO
      XVS=XKQ*VS+XDS*RKQ*IDSO
      XVC=XKQ*VC+XQS*RKQ*IQSO
      N10=-XX1*RVS
      N11=FR*RKD*XDS*RVC
      N12=VV*RD*XVS
      N13=VV*FR*XD*XVC
      N=N10-N11+N12+N13
      P10=-V*XX1*XVS
      P11=V*FR*RKD*XDS*XVC
```

```
      P12=V*RD*RVS
      P13=V*FR*XD*RVC
      P=P10-P11-P12-P13
      Q=A3*RKD*IQSD
      R=V*(XKD*A3-XAD**2)*IQSD
      S10=RKD*VC-VV*XQS*XKD*IQSD
      S11=RKD*VS-VV*XDS*XKD*IDSD
      S12=XKD*VC+XQS*RKD*IQSD
      S13=XKD*VS+XDS*RKD*IDSD
      S20=XX2*S10
      S21=FR*RKQ*XQS*S11
      S22=VV*RQ*S12
      S23=VV*FR*XQ*S13
      S=S20-S21-S22+S23
      T20=V*RQ*S10
      T21=V*FR*XQ*S11
      T22=V*XX2*S12
      T23=V*FR*RKQ*XQS*S13
      T=T20-T21+T22-T23
      H10=A1*RKQ*RKD+A2*RKQ*RKD-VV*RS*RKD*XQ
      H11=-VV*RS*RKQ*XD-VV*RQ*RD
      H12=VV*(FR**2-VV)*XQ*XD
      H=H10+H11-H12
      K10=V*RS*RKD*RQ+V*RS*RKQ*RD
      K11=V*FR**2*RKD*XDS*XQ+V*FR**2*RKQ*XQS*XD
      K12=-VV*V*RD*XQ-VV*V*RQ*XD
      K=K10+K11+K12
      W=RKQ
      X=V*XKQ
      Y=RKD
      Z=V*XKD
      CN1=CMPLX(L,M)
      CN2=CMPLX(N,P)
      CD1=CMPLX(H,K)
      CD2=CMPLX(W,X)
      CN3=CMPLX(Q,R)
      CN4=CMPLX(S,T)
      CD3=CMPLX(Y,Z)
      GJV = CN1/CD2*(CN2/CD1) + CN3/CD3*(CN4/CD1)
C
C     CALCULATE FGV
C
      FGV= WE*GJV/(2.00*HC*UP**2)
C
C
C     PRINT FGV
C
      RRG=REAL(GJV)
      AG=AIMAG(GJV)
      RFG=REAL(FGV)
      AIMFG=AIMAG(FGV)
      WRITE (6, 100) RRG, AG, RFG, AIMFG
100   FORMAT (10H          ,E12.5,5H     ,E12.5,15H                    ,E12.5
     3,5H     ,E12.5)
101   CONTINUE
      GO TO 600
C
C     IF THE SQUARE ROOT IS IMAGINARY NUMBER, THEN MACHINE WOULD BE UNSTABLE
```

```
C       THEN SKIP THE CALCULATION OF THE PLOT, PRINT OUT THAT MACHINE IS UNSTABL
C
500     WRITE (6, 505) VMM,FR,TEC
505     FORMAT (1H ,//3(5H      ,F10.7)///20H                UNSTABLE,5(/))
600     CONTINUE
C
C
C       TEC LOOP ENDS
C
        FR=FR+0.02
        IF (FR .GT. 1.20) FR=FR+0.03
        IF (FR .LT. 0.30) GO TO 30
C
C       FR LOOP ENDS
C
C
C       CHANGE VMM TO ANOTHER VALUE
C       AND CHANGE
C       THE CORRESPONDING RS AND XLS DUE TO DIFFERENT TRANSFORMER LEAKAGE
C       REACTANCES AND WINDING RESISTANCES FOR DIFFERENT VMM LEVELS
C
        IF (VMM .EQ. 1.133) GO TO 900
        IF (VMM .EQ. 1.00) GO TO 700
        VMM=1.00
        RS=0.8262
        XLS=0.8468
        XAD=10.0
        GO TO 2
700     VMM=1.133
        RS=0.8780
        XLS=0.9028
        XAD=6.7
        GO TO 2
C
C       VMM LOOP ENDS
C
900     STOP
        END
```

Average Total Computer Time For 2-Stage Search For Stability Boundaries

For each set of Machine Parameters at a Magnetic Flux Level:

0.30 Minutes CPU Time.